Warming of the Willamette River, 1850–present:

The effects of climate change and river system alterations

Stefan A.Talke[1], David A.Jay[2], Heida L. Diefenderfer[3,4]

[1]Civil and Environmental Engineering, California Polytechnic State University, San Luis Obispo, California, United States of America

[2]Civil and Environmental Engineering, Portland State University, Portland, Oregon, United States of America

[3]Coastal Sciences Division, Pacific Northwest National Laboratory, Sequim, Washington, United States of America

[4]School of Environmental and Forest Sciences, University of Washington, Seattle, Washington, United States of America

Correspondence to: Stefan A. Talke (stalke@calpoly.edu)

Keywords: Water Temperature, Climate Change, River regulation, Anthropogenic Effects

Key Points

- A statistical model based on archival records from the 1850s onwards shows that average water temperature has increased by 1.1 ^{o}C/century since the mid-19th century
- Water temperature is less variable than historically, and the deeper modern river system is less influenced by extreme heat waves or cold weather anomalies.
- Warming air temperatures are the most important factor in modeled increases in water temperature, with river system changes most influential during the cool season

Abstract

Using archival research methods, we recovered and combined data from multiple sources to produce a unique, 140-year record of daily water temperature (T_w) in the lower Willamette River, Oregon (1881–1890, 1941–present). Additional daily weather and river flow records from the 1850s onwards are used to develop and validate a statistical regression model of T_w for 1850–2020. The model simulates the time-lagged response of T_w to air temperature and river flow, and is calibrated for three distinct time periods: the late 19th, mid 20th, and early 21st centuries. Results show that T_w has trended upwards at 1.1 ºC /century since the mid-19th century, with the largest shift in January/February (1.3 ºC /century) and the smallest in May/June (~0.8 ºC /century). The duration that the river exceeds the ecologically important threshold of 20 ºC has increased by about 20 days since the 1800s, to about 60 d yr^{-1}. Moreover, cold water days below 2 ºC have virtually disappeared, and the river no longer freezes. Since 1900, changes are primarily correlated with increases in air temperature (T_w increase of 0.81 ±0.25 ºC) but also occur due to alterations in the river system such as depth increases from reservoirs (0.34 ±0.12 ºC). Managed release of water affects T_w seasonally, with an average reduction of up to 0.56 ºC estimated for September. River system changes have decreased daily variability (σ) by 0.44 ºC, increased thermal memory, reduced interannual variability, and reduced the response to short-term meteorological forcing (e.g., heat waves). These changes fundamentally alter the response of T_w to climate change, posing additional stressors on fauna.

Short Summary

We use archival measurements and a statistical model to show that average water temperature in a major US West Coast river has increased by 1.8 ºC since 1850, at a rate of 1.1 ºC /century. The largest factor driving modeled changes are warming air temperatures (nearly 75%). The remainder is primarily caused by depth increases and other modifications to the river system. Near-freezing conditions, common historically, no longer occur, and the number of warm water days has significantly increased.

1.0 Introduction

Water temperatures are rising in many temperate streams and rivers, due to climate change, land-use and development, deforestation, water withdrawal and return flows, reservoir storage, and other types of water-resources management (e.g., Kaushal et al., 2010; Olden & Naiman, 2010; Bottom et al., 2011). Assessing long-term temperature trajectories and understanding their causes is important, because water temperature (T_w) influences ecological processes, water quality, oxygen levels, and fish habitat and survivability (e.g., Caissie, 2006; Bottom et al., 2011; Clemens 2022). However, with few exceptions (e.g., Webb & Noblis, 2007; Pohle et al., 2019), few T_w records from the late 19th or early 20th century have been recovered or evaluated, particularly in North America (Kaushal et al., 2010). Historical, pre-development baselines are therefore difficult to assess, because many (often most) watershed changes, like reservoir construction, precede the start of available temperature records. Additionally, interannual and decadal variability in climate can mask or bias trends in short records (e.g., El Nino/La Nina or the Pacific Decadal Oscillation see Peterson & Kitchel, 2001; NASEM 2022). In this study, we find, recover and analyze previously forgotten or unused archival T_w records from 1881 onward for the lower Willamette River. These records, which precede most industrialization and modern development

in the Pacific Northwest, provide a unique opportunity to discern secular trends, evaluate and attribute causes, and assess the net impact of human activities in a temperate coastal river.

The changes to the Willamette River watershed over the past 150 years are substantial and mirror other regions. Like many other rivers worldwide, the Willamette River is more channelized, deeper, and reduced in length compared to 19th century conditions (e.g., Piegay et al. 2000; Ralston et al., 2019; Sedell & Froggatt, 1984; Benner & Sedell, 1997; Gregory et al., 2002a). Similar to other temperate-zone rivers, the seasonal flow regime has been altered by reduced snowpack and by the construction of flood-control and storage reservoirs (Knowles & Cayan, 2002; Cloern et al., 2011; Stewart et al., 2005; Webb & Noblis, 2007; Payne, 2002; Rounds, 2010). Beginning in the 19th century, logging within the watershed and deforestation of the riparian corridor decreased shading (Gregory et al. 1991; Johnson & Jones, 2000; Wallick et al. 2022). Urbanization, water diversions, effluent discharges, hydroelectric projects, and storage for agriculture have also likely shifted T_w (Berger et al., 2004; OR DEQ, 2006). Such processes have influenced T_w in many other regions (e.g., Nelson and Palmer, 2007; Kinouchi et al., 2007; Palmer et al., 2010). Because of a lack of in-situ data from pre-reservoir conditions, the cumulative effect of anthropogenic influence is often unknown (e.g., OR DEQ, 2006). Here, we analyze the net effect of anthropogenic stressors by developing statistical models from in-situ data that approximately represent pre-development conditions (pre-1890), post-land and river development conditions (mid-20th century), and post-reservoir management conditions (present-day).

Hydrological and land-use changes in temperate-zone river basins are occurring simultaneously with a warming climate marked by hotter extremes (e.g., Cloern et al., 2011, Hamlet & Lettenmaier, 1999; Palmer et al., 2010). Air Temperature (T_a) values in the Pacific Northwest have warmed about ~1.1 ºC since 1900 (Mote et al., 2019), and the summers of 2009, 2015, and 2021 had dry and hot conditions consistent with predictions from climate models (e.g., Mote and Salathé, 2010; Bumbaco et al., 2013). The combination of hot, dry weather and low river discharge (Mote et al., 2016) produced elevated T_w values in 2015, adversely affecting salmon populations (Crozier et al., 2020). Extreme air temperatures, however, do not always lead to extreme T_w, for reasons we investigate.

In this manuscript we investigate whether T_w averages and extremes over the past 20 years are significantly different than late 19th and mid-20th-century conditions, using much longer T_w record than previously available. From multiple, previously neglected sources we construct a unique, instrument-based T_w data set that extends back to 1881, a time period with a cooler climate and unimpeded, natural flows, before the onset of irrigation in the basin. We used a stochastic regression approach to infill data gaps back to 1850, and statistical models from different eras to attribute changes to either climate change or local factors. Our combined archival research and statistical approach provides insights into how and why temperatures are increasing in coastal rivers like the Willamette, with implications for the future response of T_w to climate change.

2. Background and Methods

2.1 Study Area

The Willamette River (Figure 1) has a 1971–2020 mean annual discharge of 940 m^3/s and drains 29,700 km^2 of coastal Oregon (Figure 1; Branscomb et al., 2002). It is the 13th largest river in the contiguous United States by volume (Wallick et al. 2022), and its waters discharge into the larger Columbia River 162km from the Pacific Ocean. The lower Willamette River, the focus of this study (Figure 1), is 43 km long. It is influenced by ocean tides most of the year, and by backwater from the Columbia River, particularly during spring (Helaire et al., 2019). Because of its location near the mouth, the lower Willamette is influenced by, and integrates climate changes and local anthropogenic changes within, its entire basin.

Evaluating changes to T_w in the Lower Willamette River is important because it influences the long-term viability of salmon and other vulnerable and endangered species (Mantua, 2010; Bottom et al., 2011, Isaak et al., 2012, Caldwell et al., 2013; Clemens 2022). Above a threshold of 18–21 ºC, various species of salmon, steelhead, and trout are stressed and become more susceptible to disease (OR DEQ, 2006, Mantua, 2010). Also, the migration and spawning of Willamette River fish such as Pacific lamprey (*Entosphenus tridentatus*) (Clemens et al. 2016) and Chinook, coho, and chum salmon (Richter and Kolmes 2005) are directly impacted by elevated temperatures. Because of such ecological effects, regulations require that the seven day average of the daily maximum temperature should not exceed 20 ºC, with a lower threshold set for rearing and spawning streams (e.g., OR-DEQ, 2006).

The Willamette Basin has a temperate climate marked by overcast conditions from October–May, and predominately dry conditions from June to September. Average annual precipitation on the valley floor is 1–1.3 m/yr., with up to 5 m occurring in mountainous headwater areas (Baker et al., 2002). Rainfall and high discharge events occur primarily between November and March (Figure 2a). Historically, snow-melt contributed to elevated flows in the March–May time frame (Figure 2a), but a combination of declining snowpack and water has reduced spring discharge (Mote et al., 2018; Rounds, 2010). During summer, 60–80% of river water derives from high-elevation regions above 1200m, either as direct snowmelt or as groundwater (Brooks et al., 2012). Late-summer discharge has increased, however, because of the managed release of water.

The mainstem of the Willamette River, which runs 300km south-to-north, has been extensively modified since the latter part of the 19th century, first for navigation and agriculture, and later for flood control. Land under irrigation was minor before 1910,but increased eightfold from 13,500 to 110,000 Ha between 1945 and 1979 (Sedell & Froggatt, 1984). Before European settlement, the river was maintained in a prairie or savannah-like condition by burning (Christy & Alverson 2011). After burning ceased (late 1700s), the river became fringed by a 3–7 km wide floodplain covered by a dense riparian forest and 2-5 shallow, braided channels (1.5-3m depth) that evolved each year (Thilenius, 1968; Sedell & Froggatt, 1984; Gregory et al., 2002a; Wallick et al. 2022). Beginning in the 1870s, but particularly in the first half of the 20th century, the river was reduced to a primarily single-thread stream, and shortened by nearly 20km (Sedell & Froggatt, 1984; Gregory et al., 2002a). Shading was much reduced (Lee et al. 1995; OR-DEQ 2006). Bank-stabilization measures began in the late 1800s and occurred most prominently during the 1930s–1960s; approximately 25% of Willamette River banks now have engineered protection (Gregory

et al., 2002b). Further, from 1870-1950, approximately 65,000 dead trees (up to 60m long with a diameter of 0.5– 2m) were removed (>500 per km; Sedell & Froggatt, 1984). As a result of these efforts, off-channel alcoves and sloughs—often 2–7 ^{o}C cooler than the mainstem—decreased in extent by 70-80% (Landers et al., 2002). Additionally, forested floodplain decreased by 75-90% (Landers et al., 2002;Gregory et al. 2019). Dredging further altered the river upstream of ~River km (Rkm) 50, particularly before 1930 (Willingham, 1983); much more extensive dredging has occurred in Portland Harbor (e.g., Helaire et al., 2019). The depth of the river is currently ~ 12m in the lower ~20km of the Willamette, the focus area of our study (Figure 1). Depths gradually reduce to a centerline depth as shallow as 1.5-2m around Rkm 280 (US Geological Survey (USGS), 2003).

A total of 371 reservoirs and impoundments have been built in the Willamette basin, with a combined capacity of more than 3.3 km^3 (Payne, 2002). Given a mean discharge of about 980 m^3s^{-1} (Naik and Jay, 2011), these reservoirs potentially store ~10.6% of the annual average flow. The majority were built between 1950–1980, with only ~23 built pre-1950 and ~25 after 1980 (Payne, 2002). Eleven federal storage and flood control reservoirs were built between 1953 and 1969 with a combined maximum storage capacity of 2.57 km^3 (Payne, 2002; Rounds, 2010). The two federal reservoirs built in the 1940s were relatively small (combined capacity of 0.18 km^3); therefore, we consider the period before 1953 to be pre-river flow regulation. Hydrological records suggests that flood control exerted some influence in the 1954–1969 period, reducing peak flows during the December 1964 flood considerably; thus, the modern hydrological regime began during this period (Waananen et al. 1970; Gregory et al., 2002c).

Reservoirs have increased the surface area of water within the system by about 200 km^2, with the majority (80–85%) occurring in the 13 federally operated water projects (Payne, 2002). An additional net increase of ~50 km^2 in water surface area is estimated for the Willamette Valley since 1851 (Gregory et al., 2002d), in part from water impoundments. By comparison, channelization between 1850 and 1995 removed ~ 17 km^2 of water surface on the mainstem Willamette, from 76 to 59 km^2 (Gregory, 2002a). Summertime peak T_w values at reservoir sites are hypothesized to have decreased after dam construction; at the same time, autumn T_w has increased (e.g., Angiletta et al., 2008; Rounds, 2010).

2.2 In situ measurements

Measurements were obtained from multiple federal, state and local archives and databases to assess meteorological and fluvial conditions between 1850–2021 (Figure 1; Table 1 & Table 2). We found and digitized previously unused records from the US Signal Service (1881-1890) and the US Weather Bureau (USWB) (1941–1961) held at the National Centers for Environmental Information (NCEI). A spot-check of US Army Corps of Engineers records from Willamette Rkm 10.5 from 1941– 42 (Moore, 1968) showed a general consistency with individual USWB measurements, to within 1^{o} C. Modern records of T_w are available from the US Geological Survey (USGS) since 1961, with ~26 station years available in the Portland metropolitan area since 1971 (Table 1). These federal records are supplemented by additional state and local records. Intermittent grab-sample measurements of T_w are available from the State of Oregon Department of Water Quality, particularly during summer (1949, 1953–present; obtained from the City of Portland). Additionally, nearly continuous daily measurements of T_w at the Willamette Falls fish

ladder from 1985– 2020 were obtained from the Oregon Department of Fish and Wildlife. Finally, continuous records were obtained for 1992–1999 and 1997–2015 at two locations near Portland (City of Portland; see also Annear et al., 2003).

We combined the above T_w records to obtain a 90-year record of in-situ T_w covering 64% of the 1881 to 2021 period (Table 1). Daily measurements were adjusted to the daily minimum temperature, because most historical measurements were made in the morning. The adjustment, typically ~0.1 ^{o}C, was based on the monthly averaged differences between measurement time stamps and the daily minimum in modern, high resolution data (Table 1). The composite 1881–2021 record uses Lower Willamette records when available, and the nearest mainstem data otherwise (if available). Records in Oregon City and farther upstream were adjusted for spatial heating effects through the use of monthly averaged gradients observed between coterminous measurements from 2000–2017. Most adjustments for spatial variability were minor (<0.3 ^{o}C), except for 1962 and 1983–1984, for which the only available measurements were from the middle or upper Willamette River. Additional notes are included in Table 1, and the sources of data in the composite are included in the data record (see data repository).

Additionally, we use T_w measurements from the lower Columbia River to check our model estimates (see section 2.4) during periods with no other data (Figure 1, Table 1). T_w was measured up to twice daily at Astoria, approximately 24 km from the ocean, from 1854–1876 (Talke et al., 2020). Monthly estimates of T_w at Tongue Point (Rkm 29) are available from 1925–1964 (U.S. Coast and Geodetic Survey (USC&GS),1967), and daily records were obtained from 1940–42 (Moore, 1968) and 1949–present from the National Oceanographic and Atmospheric Administration. Before 1950, surface waters at Astoria were generally freshwater or brackish during typical flow conditions (Al-Bahadily, 2020, USC&GS, 1967), and therefore are representative of river T_w values.

The availability and quality of in-situ data informs our choice of model calibration periods and interpretation of model/data comparisons. Monthly averages of the USGS, DEQ, and City of Portland data from 2009 to 2015 agree to within 0.1–0.2 ^{o}C, indicating that modern measurements from the last two decades are consistent and of high quality. This comparison also shows that grab samples from the water surface compare favorably with other methods. Measurements by the USSS (1881–1890) and USWB (1941–1961) were made at a 1st-order weather station by trained professionals, and appear to be of high quality; however, little independent verification is possible. Evaluation of data from 1962 to the mid-1990s indicates some periods with lesser quality in which different measurements disagree with each other. For example, summertime measurements from a thermograph in Oregon City (1963–1967) are as much as 1.8 ^{o}C higher (monthly average) than coterminous grab-samples; a smaller difference occurs between Saint Johns Bridge measurements (1971–1975) and grab-samples (Table 1). Because the typical difference between such measurements is reported to be <1 ^{o}F (0.56 ^{o}C) (Moore, 1967), an undocumented instrumental or measurement issue occurred.

2.2.1 Meteorological and Flow records

A nearly complete USGS discharge record for the lower Willamette River is available from 1893 to present, with intermittent values available from 1878–1892. Daily discharge is available from the USGS in Portland from 1972 to the present (USGS Gauge 14211720). Routed estimates of

discharge at Portland are available for earlier periods from 1878 forward from Jay & Naik (2011), based on USGS measurements at Albany (USGS Gauge 14174000) and Salem (USGS gauge 14191000).

Records of daily maximum T_a from the Portland-Vancouver area were found in several sources (Table 2). Daily USSS weather records at Vancouver (1849–1868) and Eola (1870–1892) were provided in digital form by the Midwestern Regional Climate Center (https://mrcc.purdue.edu/). Additional daily records from the USWB and the National Weather Service from Portland and Vancouver cover the 1874–present period and were obtained from NCEI.

Air temperature (T_a) records were carefully evaluated for potential bias and consistency with each other (Table 2; see Figure 1 for locations). For example, the Vancouver record from 1895–1965 averages 0.4 to 0.5 ^{o}C warmer than the downtown Portland record. Average Portland Airport values were <0.05 ^{o}C cooler than the downtown Portland Weather Bureau readings between 1940 and 1948. Thereafter, the downtown Portland record warmed more quickly, and was 0.54 ^{o}C warmer than the Airport from 1960–1969. The modern Portland KGW record (1973–present), located at 48.5m above sea-level, is slightly cooler from 1991 to 2020 (annually averaged daily maximum = 17.08 ^{o}C) than the Portland Airport (17.47 ^{o}C). Under standard atmospheric conditions, with a lapse rate 6.5 ^{o}C per 1000m, a difference of ~0.3 ^{o}C is expected between these records as compared to the actual difference of 0.39 ^{o}C. Thus, we conclude that the measured difference between the stations is almost entirely explainable by elevation effects. After adjusting for mean biases, the root-mean-square error (RMSE) between the various daily Portland T_a records is about 1-1.1 ^{o}C from 1940-present. The RMSE between Vancouver and Portland T_a is larger (1.5–1.6 ^{o}C), possibly because of small differences in local climate. The influence of these small differences on our T_w model results is explored later.

2.3 Advection-Diffusion equation

To develop our statistical model approach, understand its limitations, and motivate its form, we first consider the underlying physical dynamics. Heating and cooling of river water is governed by the Advection-Diffusion equation (ADE; e.g., Fischer et al., 1979). When vertical and cross-sectional variations in T_w are neglected, the 1-D ADE for T_w as a function of time t and along-channel coordinate x (positive downstream) reads:

$$\frac{\partial T_w}{\partial t} = \underbrace{-u\frac{\partial T_w}{\partial x}}_{Advective\ Term} + \underbrace{\frac{\partial}{\partial x}\left(K\frac{\partial T_w}{\partial x}\right)}_{Diffusive\ Term} + \underbrace{\frac{H}{\rho c_p d}}_{Heating\ term}, \quad (1)$$

where K is a horizontal diffusion coefficient, u is river velocity, H is the sum of heat flux into or out of the system, d is the cross-sectionally averaged depth, ρ is the density of water, and c_p is the heat capacity of water. This simple ADE does not consider groundwater flow, which cools the off-channel alcoves of the Willamette River during summer (Faulkner et al., 2020).

We use scaling of Equation 1 to determine the relative importance of the advection, diffusion, and heating terms, relative to the time rate of change $\frac{\partial T_w}{\partial t}$. An evaluation of measurements sug-

gests that the diffusive term is negligible, but that the nonlinear advective term is likely influential during summer, due to a positive $\frac{\partial T_w}{\partial x}$ (Figure 2). Nonetheless, the low velocities in late summer counteract the influence of large $\frac{\partial T_w}{\partial x}$. Based on our scaling, the heating term is usually the leading order term that drives the time rate of change of T_w, (c.f., Wagner et al., 2011). When advection and diffusion are unimportant, the non-linear heating term ($\frac{H}{\rho c_p d}$) drives the $\frac{\partial T_w}{\partial t}$ term. The $\frac{H}{\rho c_p d}$ term can be linearized, enabling use of a linear regression approach in which T_w is a function of T_a and river discharge Q (see Mohseni & Stefan, (1999) or the supplement for a more detailed discussion of linearization assumptions). The river discharge term incorporates the net influence of precipitation, snowmelt, and groundwater recharge.

The discussion above suggests that linear regression models have a basis in the underlying physical dynamics. However, a number of assumptions and approximations must be made to convert (1) to linear form., and a linearized representation of average conditions during a particular season may work less well under unusual or extreme conditions. Simplifying heating to be a linear function of T_a and Q works best during periods of relatively constant T_w and river discharge (see Mohseni & Stefan 1999). In summary, $\frac{\partial T_w}{\partial t}$ in (1) can be linearized and expressed in terms of three basis functions, T_w, T_a, and Q (see supplement for more information):

$$\frac{\partial T_w}{\partial t} = b_w T_w + b_a T_a - c_Q Q, \quad (2)$$

where b_w, b_a, and c_Q are coefficients and the minus sign indicates that river flow reduces T_w. Using the approximation $\frac{\partial T_w}{\partial t} \approx \frac{T_{w_n} - T_{w_{n-1}}}{\Delta t}$, we find that T_w at time step n is equal to the T_w at the previous time step (n– 1), plus a correction that is a function of T_a and Q:

$$T_{w_n} = T_{w_{n-1}} + \Delta t \left(b_w T_{w_n} + b_a T_a - c_Q Q\right) \quad (3)$$

Thus, Equations 2 & 3 depict an autoregressive (AR1) process. Hence, at time n– *1*, T_w is a function of the T_w at time n– 2, and the T_w at n– *2* depends on T_w at n– *3*. If we develop and then substitute the solutions for $T_{w_{n-1}}$, $T_{w_{n-2}}$, …. into Equation 3, we find that

$$T_w(t) = \sum_{\tau=0}^{\tau=j} a_\tau (t-\tau) T_a(t-\tau) + \sum_{\tau=0}^{\tau=j} b_\tau (t-\tau) Q(t-\tau) + C, \quad (4)$$

where a_τ and b_τ are regression coefficients at some time lag τ, C is a constant of regression, and the time period j is chosen to be long enough that the coefficients a_τ and b_τ effectively become negligible and/or statistically insignificant. Further, at the large time lag $\tau = j$, the influence of the time-lagged temperature term in Equation 3 becomes negligible and drops out. The coefficients a_τ and b_τ can be modeled using an exponential filter approach (e.g., Al-Murib et al., 2019); here, as explained below, we estimate the coefficients directly.

2.4 Statistical Model

We model Willamette River T_w by applying a stochastic modeling approach to eq. (4) (c.f., Ben-yaha et al., 2007). In this approach, the dependent variable (T_w) and the independent variables (T_A and river discharge Q) are decomposed into a long term climatological average and a time varying component. A similar approach has also been applied to the Columbia River (Scott, 2020, Scott et al., 2023); other statistical models applied to this region include Moore (1967), Donato (2002), Bottom et al. (2011) and Mayer (2012). For a generic variable *X(t)* measured daily, we define the climatological average as

$$\overline{X(t)} = \frac{1}{y_2 - y_1 + 1} \int_{y_1}^{y_2} \int_{-T/2}^{T/2} X(t) dt\, dy, \quad (5)$$

where T = 30 days, t is the integer number of days since the start of the year, y_1 is the beginning year of the time series (e.g., 1881), y_2 is the end year (e.g., 1890), and the overbar represents the climatological average. The 95% uncertainty in the climatological average is given by $\frac{t_* \sigma}{\sqrt{N}}$, where $t_* = 1.96$ for a large sample size N, and σ is the standard deviation. In practice, the number of years we used to define the climatological average is limited by available data.

The deviation from climatology, caused for example by a heat wave, is defined as:

$$X'(t) = X(t) - \overline{X(t)} \quad (6)$$

For a model to have predictive and explanatory power, it must exhibit a root mean square error (RMSE) less than $X'(t)$. Substituting Equation 5 & 6 into Equation 4, our basis function becomes:

$$T_w{}'(t) = \sum_{\tau=0}^{\tau=j} a_\tau (t-\tau) T_a{}'(t-\tau) + \sum_{\tau=0}^{\tau=j} b_\tau (t-\tau) Q'(t-\tau) + C\,, \quad (7)$$

where the prime indicates a deviation from climatology and other terms are as defined in Equation 4. Based on experimentation, we use daily $T_a{}'$ lags up to two weeks. Thereafter, we use average $T_a{}'$, to obtain a statistically significant correlation. A 15 day average is used for day 15–30, and 30 day averages are used thereafter, up to 6 months. Similarly, river discharge Q' is averaged using a 10 day average for day 1– 10, a 20 day average for day 11– 30, and – a 30 day average thereafter.

A total of 7 statistical models are developed from Equation 7, using data from the 19th century (1881–1890), mid-20th century (1941–1952), and modern period (2000–2015) (see Table 2). The models differ in the location of air temperature data and time period used. These three calibration periods were chosen based on available data; they approximate (nearly) pre-development conditions, pre-flood control conditions, and modern conditions. The models are named based on the first year of calibration data and the first letter of the meteorological station used; for example, 1941V and 1941D are models trained with 1941–1952 data from Vancouver and Downtown Portland, respectively (Table 2). Within each model, we further developed a summer sub-model (July–September), a winter sub-model (January–March) and an annual model, based on all available data. Experimentation was used to obtain the optimal timespan of winter and summer models, and the annual model is used for months not covered by the winter or summer models. For

example, the summer model covers July to September, consistent with the observation that the horizontal temperature gradient is largest during this period (Figure 2b). Through experimentation, we also determined that discharge only produces a statistically significant effect for summertime models based on 1941–1952 and 2000–2015 data (i.e., not winter or annual models).

Each statistical model produces an estimate of T_w over the period of record of its underlying T_a record (Table 2; data available as supplemental information). Based on output time series, a composite estimate of modeled T_w was produced using the best available statistical model. A compromise was required when deciding which era of model to use in the composite, because there is no absolute delineation between pre- and post-reservoir conditions, or between a nearly natural and substantially altered landscape. Models based on Vancouver T_a measurements were used pre-1868, Eola T_a measurements from 1870–1874, downtown Portland from 1874–1939, and the Portland Airport data thereafter. For each year, the two seasonal sub-models were used, with the annual sub-model used at other times. The mid-20th century calibration, representing pre-reservoir, post-landscape change conditions, was applied to the 1900–1960 period (1941A model); thereafter, we assume modern flood control, and applied the modern calibration (2000A model). Estimates from 1869–1899 used the calibration based on 1880s T_w data (1881D model). No overlap occurred between Vancouver T_a and Willamette T_w measurements during the 19th century. Hence, pre-1868 estimates used the mid-20th century calibration to Vancouver T_a (the 1941V model), since a 19th century calibration was unavailable.

The skill of each statistical model was assessed by evaluating the root-mean-square error (RMSE) between the composite model estimate and measurements. Our values are compared against the RMSE found between measurements and climatology. The uncertainty of modeled temperature estimates was assessed using a Monte Carlo approach. Two thousand possible ensembles of the model coefficients were created, under the assumption that coefficient uncertainty (obtained by the linear regression) was normally distributed. The 95th percentile of the resulting spread of solutions is reported.

2.5 Attribution Analysis

We approximate the influence of changing air temperatures, changing river discharge, and the integrated effect of river system changes through experimentation using our statistical models. The following first-order effects are approximated:

1. Climate change impacts: Climate change has driven changes in the 30 year average climatology of daily air temperature in the region (e.g., Mote et al., 2019). We estimate the influence of changed air temperature climatology by running our modern statistical model (model 2000A; see Table 2) using historical downtown climatology (1875-1904) and modern Portland airport climatology (1991-2020) (daily time scale). River flow is kept constant and does not influence results. The difference between these scenarios is attributed to climate change. The uncertainty in modeled T_w is assessed by perturbing input climatology with plausible uncertainty and bias estimates in T_a.
2. Effect of altered river flow: Changes in river flow seasonality, caused primarily by water resources management but also influenced by changing snow pack (e.g., Naik & Jay, 2011) can influence water temperatures in our 1941 and 2000 era summer models (Table

2; river flow was not statistically significant in 1881 era models). The change in the river hydrograph (see Figure 2a) is applied to the 1941 and 2000 era models (Table 2), with the T_a input kept the same between models. The difference in model output shows the influence of altered average river flow on modeled T_w for the July-September time frame between pre-reservoir (1901–1940) and modern (1981–2020) conditions.

3. Integrated system changes: Over the past 150 years, multiple landscape and watershed changes, including loss of riparian habitat and reservoir construction, have occurred (Section 2.1). We investigate their net influence on T_w by applying the same river flow and T_a data from 2000– 2020 to models from different eras (Table 2). Because the input into each statistical model is identical, any differences in output T_w are caused by changes in model coefficients (Equation 7). The uncertainty analysis in section 2.4 is applied to determine whether differences are statistically significant, consistent with the hypothesis that river system changes have altered the river's response to external heating and other forcing.

3.0 Results and Discussion

3.1 Model Assessment

Results show that the best-fit coefficients (see Equation 7) generally decrease in magnitude as T_a (Figure 3a,b,c) and river discharge (Figure 3d) are lagged backwards in time. Further, the decorrelation structure is different for the 19th, mid-20th, and 21st century models (Figure 3); hence, for the same forcing, these statistical models will produce a different output (Equation 7). Statistically significant coefficients are found at up to a 3-month lag in the 1880s model, and 4 months in the others. The magnitudes of coefficients at 2–4 month lags are larger today, at ~0.0025 $^{o}T_w/^{o}T_a$ per day (modern) vs. ~0.0017 $^{o}T_w/^{o}T_a$ per day (1940s; annual model). As discussed later, the changes in the statistical model between eras likely occurs due to the integrated effect of land use and water management changes.

Time-series comparisons of modeled and observed T_w (Figure 4) and statistical evaluations (Table 2) confirm that the stochastic model reproduces year-to-year differences in T_w and weekly–monthly perturbations caused by persistent warm/cold weather. Some synoptic scale events of less than a week are only partially captured, possibly because of factors not included in the model; e.g., cloud cover, wind, or depth changes due to backwater from the Columbia River (see also Wagner et al., 2011), and the tendency of statistical models to underestimate extremes. The RMSE between the measured and modeled daily minimum T_w varies from 0.87 to 1.1 ^{o}C for the annual model, with RMSE as low as 0.53 ^{o}C and 0.72 ^{o}C for the summertime and wintertime models, respectively (Table 2). Results are less good using Eola (1870–1892), a historical weather station which was located ~70km from Portland and may imperfectly represent local meteorological forcing. For monthly averaged estimates, RMSE varies from ~0.3 to 0.9 ^{o}C, with the best agreement obtained during the modern period and the summertime sub-models (Table 2).

Our statistical model results compare favorably with numerical models, other statistical approaches, and climatology. For example, the RMSE at Portland for a calibrated numerical model based on measurements from April–September 2002 was 0.43 ^{o}C (Berger et al., 2004), compared

to 0.52 °C for our model over the same period. Similarly, our models perform significantly better than estimates based on T_w climatology, which we calculate have a root-mean-square error (RMSE) of 1.86, 1.46, and 1.43 °C for the 1881–1890, 1941–1952, and 2000–2015 calibration periods, respectively (see Table 2). Our results compare well with traditional linear regression and stochastic models, which have reported RMSE of ~0.6–1.9 °C, depending on model type, river size and location, and averaging period (e.g., Caissie 1998; see also review by Benyahya et al., 2007 and references therein). More recent statistical models, including air2stream (Toffolon and Piccolroaz, 2015) and machine learning approaches (e.g., Fiegl et al., 2021), report RMSE of 0.5-1 °C on a daily scale, similar to the results presented here (Table 2). Results are also comparable to numerical models that generally have an RMSE <1 °C (e.g., Dugdale et al., 2017). We conclude that our statistical models accurately represent the most important factors affecting T_w, as long as the underlying measurements driving the model are reasonably accurate and representative of local conditions.

Modeled T_w estimates based on models using different T_a data series (Table 2) compare well with each other, with similar averages and variability. During their period of overlap from 1940–1973, daily modeled T_w values are slightly larger (0.08 °C) using the airport model (1941A) than the downtown Portland model (1941D). Similarly, the Vancouver model (1941V model) is 0.02 °C lower than the airport model (1941A) between 1940 and 1965. For the same periods, the daily RMSE between the 1941A model T_w and the 1941D and 1941V models is 0.29 °C and 0.32 °C, respectively. For the 1896–1965 period, the 1941D and 1941V models show a mean difference of 0.06 °C (Vancouver larger), and an RMSE of 0.37 °C. These observations provide an order of magnitude estimate of the aggregate influence of input data and model variability on uncertainty, whether caused by spatial variations in T_a, differences in the statistical coefficients, or instrumental measurement precision or bias errors. The consistency and small RMSE between model results improves our confidence in both the input data and the results.

One of the factors driving the larger RMSE in the historical model is the larger overall system variance measured for 19th century T_w. The typical distribution of T_a anomalies from the climatological mean has remained stationary between different time periods, and the standard deviation is nearly the same (within ~5%; Figure 5). However, between the 1880s and the 2000–2015 period used for calibration, the distribution of measured T_w anomalies markedly contracted, and the standard deviation decreased from 1.86 to 1.42 °C (Figure 5). Since the distribution of T_a anomalies remained similar, a likely explanation for the decreased variance in T_w is anthropogenic change to the local environment (e.g., flow regulation, landscape changes, channel deepening), namely simplification of the riverscape (Peipoch et al. 2015) (see discussion).

3.2 Water Temperature Changes in lower Willamette

Model results and measurements show that water temperatures have increased steadily since the 1800s. Increases are observed at all times of the year (Figure 6), leading to an increase in annually averaged T_w of 1.1 ± 0.2 °C/century (Figure 7). The largest increase occurred in winter; during January–February, the trend in average T_w is 1.3 ± 0.3 °C/century (Figure 6a). Similarly, the minimum annual temperature is increasing quickly, at 1.8 ± 0.5 °C/century (Figure 7b). The smallest bi-monthly averaged trends occur in late spring, during May–June (0.82 ± 0.3 °C/century trend; Figure 6d). Maximum summer temperatures are trending upwards at ~0.9 ± 0.3

°C/century (Figure 7c), smaller than the annual average. Overall, model results (grey) track available in-situ measurements (red) well, except for some months during periods with lesser data quality in the 1960s–1970s (Figure 6 & 7). The consistency of modeled and measured trends further increases confidence in our results.

No single event or individual system perturbation appears to be causing trends, as there are no step-function changes or inflection points in T_w trends (Figures 6 & 7). Instead, an upwards tendency in T_w is punctuated by large year-to-year variability. In the modern system, the largest interannual variation occurs during the typically high-flow spring (May–June), with swings of ~5 °C observed in bimonthly averages from year to year (Figure 6). The late summer and autumn season (September–December) is least variable (±1 °C variability between years). During the 19th century, greater year-to-year fluctuations occurred in both measurement and model means during all seasons, typically 4-6 °C (Figure 6). The largest decreases in year-to-year variability are observed between September to February. Cool-season measurements at Astoria (1854–1876) from November–April confirm this variability, and track modeled results despite its location on the Columbia River (see e.g. Figure 4a and 4c, Figure 6). The correspondence likely occurs because during fall and winter, proportionally more water in the lower Columbia is sourced from coastal tributaries, especially the Willamette River, than during other times of year (see Naik and Jay, 2011 and Hudson et al., 2017).

Results suggest that T_w has exceeded a threshold of 20 °C during summer for 15–90 days for the entire 1850-2021 period (Figures 4, 7c, 8 and 9), despite generally cooler 19th century conditions. A spaghetti plot of all available in-situ data shows that maximum T_w and most exceedances of the 20 °C T_w threshold have occurred in July and August (Figure 8), with no secular trend in timing observed (Figure 8, 9). During some cool summers historically (e.g., 1949; see Figure 8), T_w oscillated around 20 °C during summer. In other years, it reaches a peak of 25–26 °C and remains above the 20 °C threshold from June to September (Figures 8 & 9). During the hot, low river-discharge summers of 1889 and 2015 (Figure 8), T_w exceeded 20 °C for 91 and 95 days, respectively. The biggest difference between the two years, consistent with other observations, is that T_w was more variable during the summer of 1889 than in 2015.

Summers with persistently elevated T_w occur more often today than historically (Figures 8 & 9). On average, T_w crosses the 20 °C threshold earlier in the season and exits later than in the 1800s (Figure 9). From1881–1890, measurements show that the 7-day average temperature exceeded the effective regulatory limit of 20.3°C (a 0.3°C allowance is added to the 20°C limit; see ORDEQ, 2006) an average of 42 days, with a range of 11–80 days. For the 2000–2021 period, the range was 35– 92 days, with an average of 63 days (see also Figure 9). Thus, there is both an increased number of exceedances and a decreased (though still substantial) year-to-year variability. Evaluated using a 10-year average, the number of days per year that exceed 20 °C increased by roughly ~50% (20d) between 1850 and 2020, from around 40 d yr^{-1} to more than 60 d yr^{-1} (Figure 10). The threshold of 22 °C was exceeded relatively rarely in the 1800s (<5 days per year), but is now exceeded nearly 40 days per year.

The number of cold-water days in winter has declined as overall temperatures have warmed (Figure 10a). T_w is now rarely below 4 °C, compared to about 25 d per year in the mid-1800s. Similarly, near freezing temperatures (below 2 °C) were common in the 1800s (up to 10 d yr^{-1}), but almost never occur now.

In general, seasonal patterns of measured T_w and shifts between 19th and 21st century data are consistent with measurements of T_a, with some slight variations in timing and magnitude (Figure 11). Measurements in Portland indicate that average T_a increased by 1.3 °C between the 1875–1904 and 1991–2020 periods (based on daily maximum; Figure 11b), consistent with warming trends of 0.5–2 °C per century at 100+ stations throughout the Pacific Northwest (Mote et al., 2003). The smallest increases in Portland T_a occur in spring (April–June) and in late fall (November–December), and the largest occur in January–February and July–October, again consistent with T_a trends in the Maritime Pacific Northwest (Mote, 2003). We find little evidence that the heat-island effect (e.g., Voelkel et al., 2018) is substantially affecting these trends (see supplemental information). Regional data processed for inferred biases suggest a slightly smaller average change of 0.9 °C over a similar period (see Scott et al., 2023), and overall the Pacific Northwest increased by 1.1 °C since 1900 (Mote et al., 2023). Interestingly, the 1880s was an anomalously warm decade for both T_a and T_w; thus, T_a climatology over a 30y period shows a greater change between the 19th century and present-day (Figure 11a, 11b) than the shorter periods of T_w available for calibration (Figure 11c, 11d); see supplement.

3.3 Causes of water temperature changes

Model sensitivity tests confirm that changes in T_a driven by climate change (increased T_a) are the most significant factor in long-term increases in T_w, with net river system changes an additional important contributor during the cool season (see section 2.5, Figure 12). Seasonally, changes to T_a between the 1875–1904 and 1991–2020 periods dominate the modeled trends in T_w during late winter, summer and early fall (late January-early March, July–October; Figure 12). Averaged over a year, a total increase in T_w of 0.81 ± 0.25 °C is correlated to T_a changes. A maximum climate-induced change of ~1.7 ± 0.3 °C occurs in September. Climate shifts produce a lesser shift of 0.5–0.6 °C increase in T_w in spring (late March to June), and little change occurs in December, consistent with air-temperature climatology (compare Figure 11 and 12). The uncertainty in the T_a contribution is driven by the uncertainty in the T_a climatological average, which is ±0.22 °C and is caused by interannual variability (see Equation 5); model coefficient uncertainty is a minor factor. Modeled T_w changes are robust to small systematic biases in T_a; if the average change in T_a is reduced by 0.4 °C (consistent with the Scott et al. 2023 estimate for Portland T_a change), the average T_w only decreases by ~0.23 °C. Hence, we conclude that changes to the meteorological heat-balance (as represented by T_a) are the major cause of increasing T_w.

Integrated system changes between the 1940s and today (defined in section 2.5) cause a T_w increase of ~0.5–0.6 °C from November–May, but are statistically insignificant amount from late June to early October (Figure 12). Averaged over a year, the total increase in T_w caused by system change is 0.34 ± 0.12 °C since the 1940s; no statistically significant influence between the 1881 and 1941 era models was found, and is not shown. The net change is caused by an altered decorrelation structure between models from the 2000 and 1941 eras (Figure 3).

Changes in the average river hydrograph (Figure 2a) are important for T_w during late summer. During July, a slight increase in T_w is observed from changed river flow. In August and especially September, the decreases in T_w caused by increased flow releases (-0.27 °C and -0.56 °C, respectively) are significant. Thus, the release of water from reservoirs late in the summer to some extent counteracts the effects of increased air temperatures (Figure 12). During other times

of year, no statistically significant modeled correlation between Q and T_w was found, likely because the average T_w gradient in the mainstem Willamette River is small (Figure 2b). While river flow may be important in winter during times of large positive or negative temperature gradients, these changes are likely transient and a process-based model would be required to detect them. The net effect of summertime changes in Q on the annual average is small: a total decrease in annually averaged T_w of ~0.05 ºC is estimated.

4.0 Discussion

The observed annual trend in T_w of 1.1 ± 0.2 ºC/century in the lower Willamette River is similar to the magnitude of change observed or estimated in the few studies available over similar time scales. For example, Moatar and Gailhard (2006) estimated a 0.8 ºC increase in the Loire since 1881, Webb and Noblis (2007) estimated a change of 1.4–1.7 ºC on Austrian rivers since ~1900, and Scott et al. (2023) estimated a trend of 1.3 ºC/century for the Columbia River over the past 170 years. Similar to our results, studies also often highlight that the seasonal distribution of changes of T_w is unequal (e.g.,Webb and Noblis, 2007). Consistent with our results, studies from the Pacific Northwest suggest that the processes driving increased T_a (i.e., climate change) are also driving T_w trends over recent decades (Isaak et al., 2012). Future climate change is expected to continue to increase T_a and drive T_w trends, with the largest increases in summer (Caldwell et al., 2013; Ficklin et al., 2014). Additionally, unimpeded discharge is expected to increase in winter and decrease in summer (e.g., Chang & Jung, 2010), which would also raise late summer T_w (Figure 12).

4.1 Interpretation of T_w patterns

Ongoing air temperature changes are the primary cause of the modeled increase in water temperatures, with river system changes an important contributor (Figure 12). The sum of estimated temperature changes caused by climate, system, and water management changes from ~1900 to the present is ~1.1 ± 0.3 ºC (Figure 12) and is consistent with the overall long-term trends in T_w of 1.1 ± 0.2 ºC per century (Figure 7a). Of modeled changes since ~1900, 0.81 ± 0.25 ºC (74%) is caused by increased T_a, while 0.34 ± 0.12 ºC (~31%) is caused by alterations in the T_w response to forcing (integrated river system change); river flow alteration produces a -5% change, closing the balance. Thus, we conclude that largest increases in Willamette water temperature are driven by climate change. This contrasts with the nearby Columbia River, in which flow regulation and other anthropogenic changes cause the majority of historical T_w shifts (Scott et al., 2023). One major difference is the percentage of water that is stored in reservoirs: approximately 40% of Columbia River flow is stored behind reservoirs, vs. about 10% for the Willamette.

Our results suggest that deepening of the river system has altered the response of T_w to meteorological forcing and weather extremes, producing less water temperature variance (Figure 5 & 6) and an altered decorrelation structure in model coefficients (Figure 3). At short time lags of 0–5 days, historical model coefficients are as much as 2–3x larger than modern coefficients, indicating more sensitivity to air temperature fluctuations (Figure 3) In the modern system, increased depth d reduces the effect of atmospheric heating H, leading to smaller $\frac{\partial T_w}{\partial t}$ and smaller coefficients (see Equation 1; Caissie, 2006). Depth increases are driven by the reservoir system, which

is known to decrease T_w variability in the Willamette on 1–8 day time scales (Steel and Lange, 2007). The change from braided, shallow channels to a single, deeper channel is also likely influential (see Section 2.1).

The changing correlation structure (Figure 3) and the influence of increasing depth has implications for how extremes in a changing climate are observed. Specifically, a historical heat wave in T_a was likely to produce a larger change in T_w than it would today. The record-breaking, climate-change influenced heat wave in July 2021 (e.g., White et al., 2023), with a high T_a of 46.7 ^{o}C, did not cause a record T_w. Despite T_a values exceeding the previous all-time high by nearly 5 ^{o}C, morning water temperature peaked just over 24 ^{o}C, approximately 2 ^{o}C below the largest recorded (as discussed in section 2.2, we use morning measurements in our model). A similar process mitigates the effect of cold air events, and helps keep modern water temperatures above freezing (Figure 7). Effectively, T_w in the modern river system has become more resilient to extreme heat waves or cold weather anomalies.

Another reason for historical T_w variability in winter was the occasional occurrence of deep freezes that no longer occur. During the winters of 1861– 62 and 1867–1868, for example, T_a remained below 0 ^{o}C for 32 and 31 days, respectively, and newspapers recorded ice-skating on the lower Willamette River. Navigation in Portland Harbor was halted or hindered by ice from New Year's Day until mid-March, 1862. No 20th century winter matched the duration or severity of these events, though 18–19 freezing days (daily maximum below 0 ^{o}C) were recorded in 1915–1916, 1929–1930, and 1949–1950. In 1979, air temperatures remained below 0 ^{o}C for a total of 14 days; since 1980, no winter has produced more than 9 sub-freezing days. On average, the statistical variability of air temperature from its climatological mean is similar today as historically (Figure 5); however, the frequency of extreme cold-waves (e.g., 1 in 10 year events) has decreased over the past century (Vose et al., 2017). The average coldest day of the year is now ~2.7 ^{o}C warmer in the Pacific Northwest than during the first half of the 20th century, far outpacing the annual average increase of 1.1 ^{o}C since 1900 (Vose et al., 2017, Mote et al., 2019). Both increasing average winter air temperatures and decreasing cold extremes help explain upward trends in bi-monthly averaged temperatures (Figure 6) and seasonal minima (Figure 7b). For example, the year-to-year variation in average Jan-Feb T_w was 0-6 ^{o}C during the 19th century, and is 5-8 ^{o}C today (Figure 6). During winter, the shallower historical streams may have contributed to the ice formation observed during some 19th century winters. Thus, changing meteorological forcing combines together with altered system response to increase wintertime temperatures but reduce variance (Figure 12).

The integrated effect of weather during previous months is more important today than historically. At lags of >2 weeks, coefficient magnitudes are ~50% larger in the modern models (see section 3.1). Hence, the thermal memory of the system to T_a anomalies lasting a month or longer is larger. Nonetheless, the influence of each individual day at lags >2 weeks is small (see Figure 30, and only the integrated, monthly averaged effect is important. Hence, increased thermal memory smooths out variability and keeps the system closer to climatological conditions. Thermal memory (thermal inertia) also elevates wintertime and depresses summertime temperatures (e.g., Figure 12). Similar patterns have been observed elsewhere and attributed to water regulation and storage (see e.g. Webb & Weber, 1993; Caissie 2006; Olden and Naiman, 2010), but can be also influenced by the time-lag effects of snowmelt.

Numerical, process-based models run over a shorter duration provide additional clues to the factors driving long-term changes. For example, loss of shading (86%) and point-source discharges (~ 14%) increased Willamette River temperatures in Portland by 0.3 ±0.05 ºC between June and October of 2001 (OR DEQ, 2006). The same CE2-Qual model determined a reduction of approximately 0.1 ºC for each additional 100 m^3/s of river flow released into the lower Willamette. This is consistent though not identical with our modern statistical model, which produces an average decrease of -0.07 ºC for each extra 100 m^3/s of river flow.

River discharge is found to only be influential on T_w during summer (see also Isaak et al., 2012), and is driven by the substantial increase in water temperature along the river observed during July-September (positive $\frac{\partial T_w}{\partial x}$; Figure 2b). Another factor is the increased velocity u and river depth d caused by regulated releases of water. Larger river flow increases the rate at which cooler water is moved downstream (increased $u\frac{\partial T_w}{\partial x}$) and also diminishes the contribution from surface heating on temperature (smaller $\frac{H}{\underbrace{\rho c_p d}}$; see Equation 1). The large increase in September discharge compared to historical conditions (Figure 2) reduces temperatures by 0.56 ºC, more than in August (Figure 12). In October, average $\frac{\partial T_w}{\partial x}$ becomes small (Figure 2), and managed releases are unlikely to reduce water temperature. After September, our approach is unable to find a statistically significant influence of river discharge.

Interestingly, the overall river system was less sensitive to river flow fluctuations in the 1940s (Figure 3d), and no statistically significant effect of river flow was observed in the 1880s. The lack of correlation in the 1880s may simply reflect incomplete flow estimates (see Jay & Naik, 2011). A dynamical explanation remains speculative without a process-based retrospective model using historical bathymetry. However, some factors may have reduced average summertime river flow influences ($u\frac{dT_w}{dx}$) historically (Equation 1). Compared to today, the bottomland forests and braided river networks of the historical Willamette River probably reduced velocity u, and the longer river length slightly reduces $\frac{dT_w}{dx}$ (see section 2.1). Cold groundwater discharges, which are known to occur in off-main channel alcoves and were more connected to the river historically (e.g., Faulkner et al., 2020), may have reduced surface heating effects. Riparian shading similarly reduced heating (OR DEQ, 2006). Nonetheless, understanding the relative importance of these factors requires additional research.

4.2 Implications

The increase in the number of days that temperatures exceed established thresholds has been observed in other river systems (e.g., Markovic et al., 2013) and is projected to continue in the Pacific Northwest (Mantua, 2010). Our observations show that the rate of change is threshold-dependent, and slows as the accumulated number of days above a threshold becomes large. Therefore, the number of days over 20 ºC (which is already large) is increasing less quickly than the number of 22 ºC days, which occur primarily during mid-summer (Figure 9). Effectively, exceedances of lower thresholds like 18 ºC and 20 ºC are limited by spring and fall, when climatological values of T_z and T_w change quickly (note that spring-time T_w is also held lower by thermal

memory). Conversely, in winter, the largest rates of change are observed for larger levels of exceedance; hence, the number of cold-water days below 4 °C is decreasing faster than those below 2 °C. Both the decreased spread in water temperatures (Figure 5) and increased mean temperatures (Figure 6 & 7) drive the large change in the number of days below 4 °C. Increases in winter T_w minima and averages are not a focus of regulation, but are ecologically important (e.g., Webb & Weber, 1993; Caissie, 2006). For example, cold water events and wintertime conditions influence the survivability and recruitment of fish by altering their biotic interactions, habitat use, physical condition, feeding rates, and community structure (see reviews by Hurst 2007; Brown et al., 2011; Weber et al., 2013). It is also possible that historical wintertime conditions, such as the deep freezes discussed above, provided some protection against non-native plants and fauna that thrive in warmer waters.

Compared to historical norms, T_w today exhibits lower variability, both day-to-day and between annual maximum and minimum values. A result is that *temporal refugia*—which we define as time periods in which T_w temporarily dips below biologically important thresholds such as 18 °C or 20 °C—are becoming less frequent (see Figures 9 &10). Hence, while the management practice of selectively releasing river water is successfully reducing average temperatures in late summer (Figure 12), it may not be addressing the decrease in variance (e.g., Figure 5) caused by system changes. Because some migrating fish such as steelhead delay migration during warm periods by weeks or months, likely causing increased mortality (e.g., Siegel et al., 2021), a reduction in temporal refugia is potentially important (see also Steel et al., 2012). At Portland, T_w exceeds biologically important thresholds during some part of every year and did so even in the 19th century. However, the more consistently warm river temperatures during summer and autumn—as observed by the increase in time over 18 °C and 20 °C—likely creates a thermal barrier, with implications for salmon migration (see e.g., Notch et al., 2020).

4.3 Study Limitations

Statistical models are fast, can be applied to large time scales, and provide insights into the major factors influencing water temperature (e.g., Benyahya et al., 2007). Nonetheless, factors such as wind, heating, evaporation, time or spatial variation in parameters, and alterations in depth are only approximately represented by T_a, T_w and Q. At different times, various terms (e.g., depth, heat flux, and velocity) may contribute in varying degrees to the overall heat balance (Equation 1), leading to a different statistical relationship between forcing variables and T_w. We address this issue by developing summer, winter, and annual sub-models, and by developing models for different eras (Figure 3). Nonetheless, river system and climate changes occurred continuously over the period of record, making application of the models to different time periods only approximate. For example, managed releases of water for temperature control became more prevalent in the late 1990s (National Research Council, 2004), and may decrease the hindcast skill of our 2000 era model for earlier periods. The quality and spatial variability of input data used in the model may also affect conclusions. If we use a 0.9 °C increase in air temperature since 1900 (following Scott et al., 2023), rather than 1.3 °C, the estimated average influence of T_a on T_w is reduced by 0.23 °C in Figure 12. Nonetheless, our results are generally consistent between models (section 3.1), and any small biases or uncertainties in the data only shift the details, but not the main conclusions, of the study.

Our approach cannot discern the influence of individual factors such as altered shading, river depth, storage, or snow pack, nor can we assess coupled, nonlinear changes. For example, changes to river flow (Figure 2) may in part be caused by both climate change, land use, and water management (e.g., Swain et al., 2021, Liang et al., 2020), and alterations in T_a can be influenced by urbanization or deforestation. A numerical modeling approach is needed to isolate individual anthropogenic stressors and to determine how landscape and climate changes can influence T_w in incremental, nonlinear, and interdependent ways (e.g., Berger et al., 2004). Nonetheless, our results provide insights into the causes of T_w change and why some parts of the year are subject to larger upward trends than others, over secular timescales.

5.0 Conclusions

In this contribution, we found, digitized, produced, and quality controlled a 90-year long T_w record (1881–2021) for the lower Willamette River in Portland, Oregon. The in-situ measurements enabled the development of statistical T_w models based on the 1880s, 1940s, and modern time periods. Subsequently, estimates of daily minimum T_w for the years 1850–2021 were produced using daily measurements of maximum T_a and river discharge. A good comparison between measurements and models is observed, with RMSE similar to numerical models.

Water temperatures are increasing throughout the year (average trend of 1.1 ± 0.2 ^{o}C/ century), with the largest increase observed in winter. As a result, the number of cold-water days per year is declining, while the number of days above 20 ^{o}C has increased by an average of ~20 d yr^{-1}. The primary cause of changed T_w since ~1900 is climate change (0.84 ^{o}C), followed by system changes such as the building of reservoirs, loss of shading, and other landscape alterations (0.34 ^{o}C). Changes in river discharge have a generally smaller influence, except during managed releases in late summer.

Ongoing climate changes (as observed through air temperature increases) are the primary cause of increased water temperatures, with river system changes an important contributor, particularly during winter. Because of a larger heat capacity and greater system depth, the day-to-day variability in T_w has decreased and the sensitivity to meteorological heat waves or cold waves is diminished. These changes are observed in model coefficients and in a reduced variance from the climatological mean. Thus, average temperatures in summer are now higher than historically and have increased more rapidly than annual maxima. Hence, warm summers marked by low river flow produced similar peak temperatures in 1889, 1941, and 2015, but an extreme heat wave in 2021 did not produce record T_w values. River system alterations and climate change have greatly increased winter temperatures and reduced year-to-year variability, and meteorologically induced disturbance events such as freezing rarely occur anymore. Similarly, temporal refugia—time periods in which T_w dips below biologically important warm water thresholds—have also decreased. These system changes may pose a grave threat to endemic species, should climate-induced changes in T_w continue.

Data Availability

The T_w data have been archived in the Portland State University data depository (https://doi.org/10.15760/cee-data.06). Meteorological data are available from the National Centers for Environmental Information (https://www.ncei.noaa.gov/). Pre-1890 Vancouver and Portland records were also obtained from the Midwestern Regional Climate Center (https://mrcc.illinois.edu/data_serv/cdmp/cdmp.jsp). River flow records are obtained from the US Geological Survey and the sources described in section 2.2.

Author Contribution

SAT found and processed archival data, conceptualized research question, developed the statistical model, analyzed results, produced figures, and was primary lead on drafting the paper. DAJ developed an earlier version of the model and assisted with research questions, interpretation and paper development. HLD assisted with conceptualizing research questions, interpretation, literature review, and paper development.

Competing Interests

The authors declare that they have no conflict of interest

Acknowledgements

Funding was provided by Bonneville Power Administration, under Project No. 2002-077-00 with the Pacific Northwest National Laboratory, and by the US National Science Foundation, CAREER Award 1455350 and NSF project 2013280. Margaret McKeon is thanked for her help defining the watershed boundaries in Figure 1, and students at Portland State University are thanked for helping to digitize and quality assure the 1854-1876, 1881-1890, and 1941-1961T_w records used in this study.

References

Al-bahadily, A.: Long Term Changes to the Lower Columbia River Estuary (LCRE) Hydrodynamics and Salinity Patterns. PhD thesis. Portland State University, doi: 10.15760/etd.7357, 2020.

Al-Murib, M. D., Wells, S. A., and Talke, S. A.: Integrating Landsat TM/ETM+ and numerical modeling to estimate water temperature in the Tigris River under future climate and management scenarios. Water, 11(5), 892, doi.org/10.3390/w11050892, 2019.

Angilletta M.J., Steel E.A., Bartz K.K., Kingsolver J.G.,Scheurell M.D., Beckman B.R., and Crozier L.G.: Big dams and salmon evolution: changes in thermal regimes and their potential evolutionary consequences. Evolutionary Applications,1, 286–299, doi: 10.1111/j.1752-4571.2008.00032.x, 2008.

Annear, R., McKillip, M., Khan, S. J., Berger, C., and Wells, S.: Willamette Basin Temperature TMDL Model: Boundary Conditions and Model Setup, Technical Report EWR-03-03, Department of Civil and Environmental Engineering, Portland State University, Portland, Oregon, 2003.

Baker, J., Van Sickle, D., White, D.: Water Sources and Allocation. In: Willamette River Basin Planning Atlas (D. Hulse, S. Gregory and J. Baker, Eds.), pp. 40–43. Oregon State University Press, Corvallis, 2002.

Benyahya L., Caissie,D.,St-Hilaire, A., Ouarda, T.B.M.J., and B. Bobée.: A Review of statistical water temperature models. Canadian Water Resources Journal, 32(3), 179-192, doi.org/10.4296/cwrj3203179, 2007.

Benner, P., and Sedell, J.: Upper Willamette River Landscape: A Historic Perspective. In River Quality: Dynamics and Restoration. Ed. Antonius Laenen and David A. Dunnette. Boca Raton: CRC/Lewis, 23-46, 1997.

Berger, C., McKillip, M.L., Annear, R.L., Khan, S.J., and Wells, S.A.: Willamette Basin Temperature TDML Model: Model Calibration. Portland State University, Department of Civil and Environmental Engineering. Technical Report EWR-02-04, 2004.

Branscomb,A., Goicochea J., and Richmond, M.: Stream Network. In: Willamette River Basin Planning Atlas (D. Hulse, S. Gregory and J. Baker, Eds.), 16-17, Oregon State University Press, Corvallis, 2002.

Brooks, J. R., Wigington, P. J., Phillips, D. L., Comeleo, R., and Coulombe, R.: Willamette River Basin surface water isoscape (δ 18O and δ 2H): temporal changes of source water within the river, Ecosphere, 3, 39, doi:10.1890/ES11-00338.1, 2012.

Brown, R. S., Hubert, W. A., and Daly, S. F.: A primer on winter, ice, and fish: what fisheries biologists should know about winter ice processes and stream-dwelling fish, Fisheries, 36(1), 8-26, doi.org/10.1577/03632415.2011.10389052, 2011.

Bumbaco, K. A., Dello, K.D., and Bond, N.A.: History of Pacific Northwest Heat Waves: Synoptic Pattern and Trends. Journal of Applied Meteorology and Climatology, DOI:10.1175/JAMC-D-12-094.1, 2013.

Bottom, D., Baptista, A., Burke, J., Campbell, L., Casillas, E., Hinton, S., Jay, D.A., Lott, M. A., McCabe, G., McNatt, R., Ramirez, M., Roegner, G. C., Simenstad, C. A., Spilseth, S., Stamatiou, L., Teel, D. and Zamon, J. E.: Estuarine habitat and juvenile salmon: Current and historical linkages in the Lower Columbia River and estuary. Final report, 2002-2008. Report of the National Marine Fisheries Service to the U.S. Army Corps of Engineers. Portland, Oregon. Available at https://www.nwfsc.noaa.gov/publications/index.cfm, 2011.

Boyd, Robert, ed. Indians, Fire, and the Land in the Pacific Northwest: Corvallis: Oregon State University Press, 1999.

Caissie, D., El-Jabi, N. and St-Hilaire, A.: Stochastic Modelling of water temperatures in a Small Stream Using Air to Water Relations. Canadian Journal of Civil Engineering, 25, 250–260, doi.org/10.1139/l97-091, 1998.

Caissie, D.: The thermal regime of rivers: a review. Freshwater Biology, 51, 1389-1406, doi.org/10.1111/j.1365-2427.2006.01597.x, 2006.

Caldwell, R.J., Gangopadhyay, S., Bountry, J., Lai, Y. and Elsner, M.M.: Statistical modeling of daily and subdaily stream temperatures: Application to the Methow River Basin, Washington, Water Resources Research, 49, 4346 – 4361, doi.org/10.1002/wrcr.20353, 2013.

Chang, H., and Jung, I. W.: Spatial and temporal changes in runoff caused by climate change in a complex large river basin in Oregon, Journal of Hydrology, 388(3), 186-207, doi.org/10.1016/j.jhydrol.2010.04.040, 2010.

Christy, J.A. and Alverson, E.R.: Historical vegetation of the Willamette Valley, Oregon, circa 1850. Northwest Science, 85(2), 93-107, https://doi.org/10.3955/046.085.0202, 2011

825 Clemens B, Schreck C, van de Wetering S, and Sower S.: The potential roles of river environ-
826 ments in selecting for stream- and ocean-maturing Pacific lamprey, Entosphenus tridenta-
827 tus (Gairdner, 1836). Pages 299– 322 in Orlov A, Beamish R, editors. Jawless fishes of
828 the world. Volume 1. Newcastle upon Tyne, UK: Cambridge Scholars Publishing.
829 Clemens, B. J.: Warm water temperatures (≥ 20°C) as a threat to adult Pacific lamprey: Implica-
830 tions of climate change. Journal of Fish and Wildlife Management 13:1–8,
831 DOI:10.3996/JFWM-21-087, 2022
832 Cloern, J. E., N. Knowles , L. R. Brown, D. Cayan , M. D. Dettinger , T. L. Morgan , D. H.
833 Schoellhamer, M. T. Stacey , M. van der Wegen , R. W. Wagner, and A. D. Jassby.: Pro-
834 jected evolution of California's San Francisco Bay-Delta-River System in a century of
835 climate change, PLoS ONE, 6(9), e24465, doi:10.1371/journal.pone. 0024465, 2011.
836 Crozier, L. G., Siegel, J. E., Wiesebron, L. E., Trujillo, E. M., Burke, B. J., Sandford, B. P., and
837 Widener, D. L.: Snake River sockeye and Chinook salmon in a changing climate: impli-
838 cations for upstream migration survival during recent extreme and future climates. PloS
839 one, 15(9), e0238886, doi.org/10.1371/journal.pone.0238886, 2020.
840 Donato, M.M.: A Statistical Model for Estimating Stream Temperatures in the Salmon and
841 Clearwater River Basins, Central Idaho. US Geological Survey Water Resources Investi-
842 gations Report 2002-4195, 2002.
843 Dugdale, S. J., Hannah, D. M., and Malcolm, I. A.: River temperature modelling: a review of
844 process-based approaches and future directions, Earth Sci. Rev. 175, 97–113. doi:
845 10.1016/j.earscirev.2017.10.009, 2017.
846 Erickson, T. R. and Stefan, H. G.: Linear air/water temperature correlation for streams during
847 open water periods. Journal of Hydrologic Engineering, 5(3), 317-321,
848 doi.org/10.1061/(ASCE)1084-0699(2000)5:3(317), 2000.
849 Faulkner B.R., Brooks J.R., Keenan D.M., and Forshay K.J.: Temperature Decrease along
850 Hyporheic Pathlines in a Large River Riparian Zone, Ecohydrology. 13(1), 1-10, doi:
851 10.1002/eco.2160. PMID: 32983317; PMCID: PMC7513865, 2020.
852 Ficklin, D. L., Barnhart, B. L., Knouft, J. H., Stewart, I. T., Maurer, E. P., Letsinger, S. L. and
853 Whittaker, G. W.: Climate change and stream temperature projections in the Columbia
854 River basin: habitat implications of spatial variation in hydrologic drivers, Hydrol. Earth
855 Syst. Sci., 18, 4897–4912, https://doi.org/10.5194/hess-18-4897-2014, 2014.
856 Fischer, H.B., List, E.J., Koh, R.C.Y., Imberger, J., and Brooks, N.H.: Mixing in inland and
857 coastal waters. New York: Academic, 1979.
858 Gregory, S., Ashkenas, L., Oetter, D., Minear, P., and Wildman, K.: Historical Willamette River
859 Channel Change. In: Willamette River Basin Planning Atlas (D. Hulse, S. Gregory and J.
860 Baker, Eds.), pp. 18-25. Oregon State University Press, Corvallis, 2002a.
861 Gregory, S., Ashkenas, L., Oetter, D. Wildman, R,, Minear, P., Jett, S., and Wildman, K.: Revet-
862 ments, In: Willamette River Basin Planning Atlas (D. Hulse, S. Gregory and J. Baker,
863 Eds.), pp. 32–33. Oregon State University Press, Corvallis, 2002b.
864 Gregory, S., Ashkenas L., Jett, S., and Wildman, R.: Flood inundations/FEMA floodplains. In:
865 Willamette River Basin Planning Atlas (D. Hulse, S. Gregory and J. Baker, Eds.), pp. 28–
866 29. Oregon State University Press, Corvallis, 2002c.
867 Gregory, S., Ashkenas L., Oetter,D., Minear, P., Wildman, K., Christy, J., Kolar, S., and Alver-
868 son, E.: Presettlement Vegetation ca. 1851. In: Willamette River Basin Planning Atlas
869 (D. Hulse, S. Gregory and J. Baker, Eds.), pp. 38–39. Oregon State University Press, Cor-
870 vallis, 2002d.

Gregory, S., Ashkenas, L., Haggerty, P., Oetter, D. Wildman, K,, Hulse, D., Branscomb, A. and Van Sickle, J.: Riparian vegetation, In: Willamette River Basin Planning Atlas (D. Hulse, S. Gregory and J. Baker, Eds.), pp. 40–43. Oregon State University Press, Corvallis, 2002e.

Gregory, S.V., Frederick J. Swanson, W. Arthur McKee, Kenneth W. Cummins, An Ecosystem Perspective of Riparian Zones: Focus on links between land and water, BioScience, 41(8), 540–551, https://doi.org/10.2307/1311607, 1991.

Gregory, S., Wildman, R., Hulse, D., Ashkenas, L. and Boyer, K.: Historical changes in hydrology, geomorphology, and floodplain vegetation of the Willamette River, Oregon, River Research and Applications, 35(8), 1279-1290, https://doi.org/10.1002/rra.3495, 2019.

Hamlet, A. F. and Lettenmaier, D. P.: Effects of climate change on hydrology and water resources in the Columbia River Basin, JAWRA Journal of the American Water Resources Association, *35*(6), 1597-1623, https://doi.org/10.1111/j.1752-1688.1999.tb04240.x, 1999.

Helaire, L.T., Talke, S.A., Jay, D. A. and Mahedy, D.: Historical changes in Lower Columbia River and Estuary Floods and Tides. Journal of Geophysical Research, 124(11), https://doi.org/10.1029/2019JC015055, 2019.

Hudson, A.S., Talke, S.A., and Jay, D.A.: Using satellite observations to characterize the response of estuary turbidity maxima to external forcing, Estuaries and Coasts, 39(5), DOI 10.1007/s12237-016-0164-3, 2017.

Hurst, T. P.: Causes and consequences of winter mortality in fishes, Journal of Fish Biology, 71(2), 315-345, doi.org/10.1111/j.1095-8649.2007.01596.x, 2007.

Jay, D.A., and Naik, P.K.: Distinguishing Human and Anthropogenic Influences on Hydrological Disturbance Processes in the Columbia River, USA. Hydrological Sciences Journal, 56(7), 1186-1209, https://doi.org/10.1080/02626667.2011.604324, 2011.

Johnson S.L. and Jones J.A.: Stream temperature response to forest harvest and debris flows in western Cascades, Oregon. Canadian Journal of Fisheries and Aquatic Sciences, 57 (Suppl. 2), 30–39, doi.org/10.1139/cjfas-57-S2-30, 2000.

Kaushal, S. S., Likens, G. E., Jaworski, N. A., Pace, M. L., Sides, A. M., Seekell, D., Belt, D.H., Secor, R.L., and Wingate, R. L.: Rising stream and river temperatures in the United States. Frontiers in Ecology and the Environment, 8(9), 461-466, doi.org/10.1890/090037, 2010.

Kinouchi, T.: Impact of long-term water and energy consumption in Tokyo on wastewater effluent: implications for the thermal degradation of urban streams. Hydrol. Process. 21, 1207–1216. DOI: 10.1002/hyp.6680, 2007.

Knowles, N. and Cayan, D.: Potential Effects of Global Warming on the Sacramento/SanJoaquin Watershed and the San Francisco Estuary, Geophys. Res. Lett. 29, https://doi.org/10.1029/2001GL014339, 2002.

Landers D., Fernald A., Andrus C.: Off-channel Habitats. In: Willamette River Basin Planning Atlas (D. Hulse, S. Gregory and J. Baker, Eds.), pp. 26-27. Oregon State University Press, Corvallis, 2002.

Lee, K.: Stream Velocity and Dispersion Characteristics Determined by Dye-Tracer Studies on Selected Stream Reaches in the Willamette River Basin, Oregon. U.S. Geological Survey Water-Resources Investigations Report 95–4078, 1995.

Liang, S., Wang, W., Zhang, D., Li, Y., & Wang, G.: Quantifying the impacts of climate change and human activities on runoff variation: case study of the upstream of Minjiang River, China. Journal of Hydrologic Engineering, 25(9), 05020025, 2020.

Mantua, N., Tohver, I., and Hamlet, A.: Climate change impacts on streamflow extremes and summertime stream temperature and their possible consequences for freshwater salmon habitat in Washington State. Climatic Change, 102(1), 187-223, https://doi.org/10.1007/s10584-010-9845-2, 2010.

Markovic, D., Scharfenberger, U., Schmutz, S., Pletterbauer,F., and Wolter, C.: Variability and alterations of water temperatures across the Elbe and Danube River Basins. Climatic Change 119, 375–389, doi.org/10.1007/s10584-013-0725-4, 2013.

Mayer, T.D.: Controls of summer stream temperature in the Pacific Northwest. Journal of Hydrology, 475, 323-335. https://doi.org/10.1016/j.jhydrol.2012.10.012, 2012.

Monthly Weather Review (MWR): American Meteorological Society, Online ISSN: 1520-0493, Volume 9 to 17, 1881-1889.

Moore, A. M.: Correlation and analysis of water temperature data for Oregon Streams. United States Geological Survey Water-Supply Paper 1818-K, 53 pages, 1967.

Moore, A. M.: Water temperatures in the lower Columbia River. United States Geological Survey, Circular 551, doi.org/10.3133, 1968.

Mote, P.W.: Trends in temperature and precipitation in the Pacific Northwest during the twentieth century. Washington State University, 2003.

Mote, P.W., Parson E. A., Hamlet, A. F. , Keeton, W. S. , Lettenmaier D., Mantua, N, Miles, E. L., Peterson, D. W.,. Peterson, D. L, Slaughter, R., and Snover, A.K.: Preparing for Climatic Change: The Water, Salmon, and Forests of the Pacific Northwest. Climatic Change 61, no. 1-2, 45-88, doi.org/10.1023/A:1026302914358, 2003.

Mote, P. W., and Salathé, E. P.: Future climate in the Pacific Northwest. Climatic change, 102(1), 29-50, doi.org/10.1007/s10584-010-9848-z, 2010.

Mote, P.W., Rupp, D.E., Li, S., Sharp, D.J., Otto, F., Uhe, P.F., Xiao, M., Lettenmaier, D.P., Cullen, H. and Allen, M. R.: Perspectives on the cause of exceptionally low 2015 snowpack in the western United States, Geophysical Research Letters, 43, doi:10.1002/2016GLO69665, 2016.

Mote, P. W., Li, S., Lettenmaier, D. P., Xiao, M., and Engel, R.: Dramatic declines in snowpack in the western US. Npj Climate and Atmospheric Science, doi:10.1038/s41612-018-0012-1, 2018.

Mote, P.W., Abatzoglou, J., Dello, K.D., Hegewisch, K., and Rupp, D.E.: Fourth Oregon Climate Assessment Report. Oregon Climate Change Research Institute. occri.net/ocar4; accessed online February 4, 2019, 2019.

Naik, P. K. and D. A. Jay.: Human and climate impacts on Columbia River hydrology and salmonids, River Research and Applications, 27, 1270-1276, DOI:10.1002/rra.1422, 2011.

National Research Council.: Managing the Columbia River: Instream Flows, Water Withdrawals, and Salmon Survival, Washington, DC: The National Academy Press. https://doi.org/10.17226/10962, 2004.

National Academies of Sciences, Engineering, and Medicine 2022. An Approach for Assessing U.S. Gulf Coast Ecosystem Restoration: A Gulf Research Program Environmental Monitoring Report. Washington, DC: The National Academies Press. https://doi.org/10.17226/26335

Nelson, K. C., & Palmer, M. A: Stream temperature surges under urbanization and climate change: data, models, and responses, JAWRA journal of the American water resources association, 43(2), 440-452, https://doi.org/10.1111/j.1752-1688.2007.00034.x, 2007.

Notch, J.J., McHuron, A.S., Michel, C.J. , Cordoleani, F., Johnson M., Henderson, M.J. and Ammann, A.J.: Outmigration survival of wild Chinook salmon smolts through the Sacramento River during historic drought and high water conditions. Environ Biol Fish 103, 561–576. https://doi.org/10.1007/s10641-020-00952-1, 2020.

Olden J. D. and R. J. Naiman.: Incorporating thermal regimes into environmental flows assessments: modifying dam operations to restore freshwater ecosystem integrity, Freshwater Biology, 55, 86–107, doi.org/10.1111/j.1365-2427.2009.02179.x, 2010.

Oregon Department of Environmental Quality (OR-DEQ): Willamette Basin TMDL and WQMP. Chapter 4: Temperature-Mainstem TDML and subbasin Summary. Accessed from https://www.oregon.gov/deq/wq/tmdls/Pages/willamette2006.aspx, accessed 2021-08-21, 2006.

Palmer, M. A., Lettenmaier, D. P., Poff, N. L., Postel, S. L., Richter, B., & Warner, R.: Climate change and river ecosystems: protection and adaptation options, Environmental management, 44, 1053-1068, https://doi.org/10.1007/s00267-009-9329-1, 2009.

Payne, S. K.: Dams. In: Willamette River Basin Planning Atlas (D. Hulse, S. Gregory and J. Baker, Eds.), pp. 30-31. Oregon State University Press, Corvallis, 2002.

Petersen, J. and Kitchell, J.: Climate regimes and water temperature changes in the Columbia River: Bioenergetic implications for predators of juvenile salmon, Canadian Journal of Fisheries and Aquatic Sciences, 58, 1831-1841. 10.1139/cjfas-58-9-1831, 2001.

Piegay, H., Bornette G., Citterio A., Herouin, E., Moulin, B., and Statiotis, C.: Channel instability as a control on silting dynamics and vegetation patterns within perifulvial aquatic zones. Hydrological Processes 14: 3011-3029, 2000.

Peipoch, M., Brauns, M., Hauer, F.R., Weitere, M. and Valett, H.M.: Ecological simplification: human influences on riverscape complexity. BioScience, 65(11), pp.1057-1065, 2015.

Pohle I., Helliwell, R., Aube, C., Gibbs, S., Spencer, M. and Spezia, L.: Citizen science evidence from the past century shows that Scottish rivers are warming, Sci. Tot. Envr. 10.1016/j.scitotenv.2018.12.325, 2019.

Ralston, D.K., Talke, S.A., Geyer, W. R., Al'Zubadaei H., and Sommerfield, C. K.: Bigger tides, less flooding: Effects of dredging on water level in the Hudson River estuary, Journal of Geophysical Research, 124(1), doi: 10.1029/2018JC014313, 2019.

Richter, A. and Kolmes,S.A.: Maximum temperature limits for Chinook, coho, and chum salmon, and steelhead trout in the Pacific Northwest. Reviews in Fisheries Science 13:23-49, DOI: 10.1080/10641260590885861, 2005.

Rounds, S.A.: Thermal effects of dams in the Willamette River basin, Oregon: U.S. Geological Survey Scientific Investigations Report 2010-5153, 64 p, 2010.

Rounds, S.A.: Temperature effects of point sources, riparian shading, and dam operations on the Willamette River, Oregon: U.S. Geological Survey Scientific Investigations Report 2007-5185, 34 p. (Also available at http://pubs.usgs.gov/sir/2007/5185.), 2007.

Scott, M.H.: Statistical Modeling of Historical Daily water temperatures in the Lower Columbia River. Master of Science Thesis, Civil and Environmental Engineering, Portland State University, Portland, OR, USA, 2020. https://doi.org/10.15760/etd.7466

Scott, M.H., Talke, S.A., Jay, D.A. and Diefenderfer, H.: Warming of the Columbia River, 1853 to 2018. River Research and Applications, 2023 (Accepted with minor revisions).

Sedell, J.R. and Froggatt, J.L.: Importance of streamside forests to large rivers: The isolation of the Willamette River, Oregon, USA, from its floodplain by snagging and streamside forest removal, Internationale Veriningung fur Theoretische and Angewandte Limnologie Verhandlungen (International Association for Theoretical and Applied Limnology) 22, 1828–1834, 1984.

Steel, E. A., and Lange, I. A.: Using wavelet analysis to detect changes in water temperature regimes at multiple scales: Effects of multi-purpose dams in the Willamette River basin, River Research and Applications, 23(4), 351-359, doi.org/10.1002/rra.985, 2007.

Steel, E. A., Tillotson, A., Larsen, D. A., Fullerton, A. H., Denton, K. P., & Beckman, B. R.: Beyond the mean: the role of variability in predicting ecological effects of stream temperature on salmon, Ecosphere, 3(11), 1-11, doi.org/10.1890/ES12-00255.1, 2012.

Swain, S. S., Mishra, A., Chatterjee, C., & Sahoo, B.: Climate-changed versus land-use altered streamflow: A relative contribution assessment using three complementary approaches at a decadal time-spell, Journal of Hydrology, 596, https://doi.org/10.1016/j.jhydrol.2021.126064, 2021.

Talke, S.A., Mahedy, A., Jay, D.A., Lau, P. Hilley, C., and Hudson,A.: Sea level, tidal and river flow trends in the Lower Columbia River Estuary, 1853-present, Journal of Geophysical Research-Oceans. https://doi.org/10.1029/2019JC015656, 2020.

Taylor, J.E.: Making Salmon: An Environmental History of the Northwest Fisheries Crisis. University of Washington Press, 488pp, 1999.

Thilenius, J.F., 1968. The Quercus garryana forests of the Willamette valley, Oregon. Ecology, 49(6), 1124-1133.

Toffolon, M. and Piccolroaz, S.: A hybrid model for river water temperature as a function of air temperature and discharge, Environ. Res. Lett., 10, 114011, https://doi.org/10.1088/1748-9326/10/11/114011, 2015.

USC&GS (US Coast and Geodetic Survey): Surface water temperature and Density, Pacific Coast North and South America & Pacific Ocean Islands. U.S. Government Printing Office, Rockville, Maryland, 1967.

USGS (United States Geological Survey): Willamette River Bathymetric Survey – Willamette River water temperature Investigation. Retrieved July 28, 2022. https://or.water.usgs.gov/projs_dir/will_tmdl/main_stem_bth.html, 2003.

Voelkel J. , Hellman D., Sakuma R., and Shandas V.: Assessing Vulnerability to Urban Heat: A Study of Disproportionate Heat Exposure and Access to Refuge by Socio-Demographic Status in Portland, Oregon, International Journal of Environmental Research and Public Health, DOI: 10.3390/ijerph15040640, 2018.

Vose, R.S., Easterling, D.R., Kunkel, K.E., LeGrande, A.N. & Wehner, M.F.: Temperature changes in the United States. In: Climate Science Special Report: Fourth National Climate Assessment, Volume I [Wuebbles, D.J., D.W. Fahey, K.A. Hibbard, D.J. Dokken, B.C. Stewart, and T.K. Maycock (eds.)]. U.S. Global Change Research Program, Washington, DC, USA, pp. 185-206, doi: 10.7930/J0N29V45, 2017.

Waananen, A. O., Harris, D. D., & Williams, R. C. (1970). *Floods of December 1964 and January 1965 in the Far Western States; Part 1 Description* and *Part 2 Stream flow and sediment data* (US Geological Survey Water Supply Papers 1866A&B), Washington, D.C.

Wagner, R. W, Stacey, M.T., Brown, L.R. and Dettinger. M.: Statistical models of temperature in the Sacramento-San Joaquin delta under climate-change scenarios and ecological implications, Estuaries and Coasts, 34: 544-556, https://doi.org/10.1007/s12237-010-9369-z, 2011.

Wallick, J.R., Grant, G., Lancaster, S., Bolte, J.P. and Denlinger, R.: Patterns and controls on historical channel change in the Willamette River, Oregon USA. Large Rivers: Geomorphology and Management, Second Edition, pp.737-775, 2022.

Webb B.W. and Walling D.E.: Temporal variability in the impact of river regulation on thermal regime and some biological implications, Freshwater Biology, 29, 167–182, doi.org/10.1111/j.1365-2427.1993.tb00752.x 1993.

Webb, B. W., Clack, P.D., and Walling, D.E.: Water-air temperature relationships in a Devon river system and the role of flow, Hydrological Processes, 17, 3069-3084, https://doi.org/10.1002/hyp.1280, 2003.

Webb, B. W. and Nobilis, F.: Long-term changes in river temperature and the influence of climatic and hydrological factors, Hydrological Sciences Journal, 52(1): 74-85, doi.org/10.1623/hysj.52.1.74, 2007.

Weber, C., Nilsson, C., Lind, L., Alfredsen, K. T., and Polvi, L. E.: Winter disturbances and riverine fish in temperate and cold regions, BioScience, 63(3), 199-210, doi.org/10.1525/bio.2013.63.3.8, 2013.

White, S.M., Justice, C. Kelsey, D.A., McCullough, D.A. and Smith, T.: Legacies of stream channel modification revealed using General land Office surveys, with implications for water temperature and aquatic life, Elementals: Science of the Anthropocene 5(3). https://doi.org/10.1525/elementa.192, 2017.

White, R.H., Anderson, S., Booth, J.F. *et al.*: The unprecedented Pacific Northwest heatwave of June 2021. *Nat Commun* 14, 727, https://doi.org/10.1038/s41467-023-36289-3, 2023.

Willingham, W.F.: Army Engineers and the Development of Oregon. United States Army Corps of Engineers, Portland, 259 pp, 1983.

Zhu, S, Nyarko, E.K., and Hadzima-Nyarko, M.: Modelling daily water temperature from air temperature for the Missouri River. PeerJ, https://doi.org/10.7717/peerj.4894, 2018.

Tables and Figures

Table 1: In-situ T_w measurements used to obtain a composite record of daily minimum in Portland, 1881– 2021. Locations ordered based on start-date and originating agency. Precision based on measurement significant figures. A bias correction was applied to standardize measurements to the daily minimum T_w, based on the time of day of the measurement, and to account for the T_w gradient between Portland and upstream stations. River kilometers (km) from the mouth are indicated for the Columbia River (CR) and the Willamette River (WR). Additional information on the data used in the composite in situ T_w series is included in the data repository.

Location	Originating agency	Short name	River km	Latitude	Longitude	Measurement Dates	Measurement Frequency	Precision	Bias Correction	Dates used in composite T_w
Astoria Downtown[a]	US Coast Survey	A1	CR 24	46.19	-123.829	6/1854– 10/1876	Various, usually 6:00 am and 6:00 pm daily	±0.03 ºC	None applied	
Stark Street, Portland[b]	US Signal Service	S1	WR-21	45.519	-122.671	9/1881 – 11/1890	11:00 am daily	±0.3 ºC	0.1 ºC to 0.2 ºC	1881-1890
Astoria Tongue Point	US CGS (pre-1973) & NOAA	A2	CR 29	46.207	-123.768	1/1925– present; daily to 1995, hourly 1995– present	Monthly 1/1925– 12/1964; Daily 11/1940– 6/1942, 01/1949– 12/1995; Hourly 11/1993– present	±0.2 ºC before 1994; ±0.03 ºC modern	None applied	
Morrison Street Bridge, Portland[b]	US Weather Bureau	W1	WR-21	45.517	-122.668	7/1941 – 10/1961	7:30 am daily (except Sunday)	±0.3 ºC	0 ºC to 0.2 ºC	1941-1961
Lower Willamette River[d]	Oregon Department of Environmental Quality	D1	WR-19–21 (primarily)	Various	Various	1949– 2015; 2746 grab samples retained after quality assurance	6:00am– 12:00 pm; mode = 9:00 am. monthly in winter, once weekly in summertime	±0.1 ºC	Median 0.1 ºC; 90% corrections < 0.2 ºC	1963-1974
Harrisburg	USGS Gauge 14166000	HA	WR-259	44.2704	-123.174	6/1961– 9/1987 10/2000– Present	Daily Max, Min & Mean	±0.05 ºC	Spatial gradient correction, June-September	1961-1963, 1982-1984
Oregon City	USGS Gauge 14207770	U2	WR-42	45.3578	-122.610	3/1963– 9/1967	Daily Max, Min & Mean	±0.05 ºC	0.7– 1.8ºC Diff. w/Grab samples during summer	1963-1967
Salem	USGS Gauge 14191000	SA	WR-137	44.9442	123.0429	10/1963 – 9/1987	Daily Max, Min & Mean	±0.05 ºC		1981-1982
Saint Johns Bridge	USGS Gauge 14211805	U3	WR-9	45.583	-122.759	10/1971– 9/1975	Daily Max, Min & Mean	±0.05 ºC	0.6– 1.05 ºC Diff. w/Grab samples during summer	1971-1975
Morrison Street Bridge, Portland	USGS Gauge 14211720	U1	WR-21	45.5175	-122.669	11/1975– 9/1981 11/2001–9/2005 01/2009– 2021	Daily Max, Min & Mean through 2005. Every 30 minutes	±0.05 ºC	None applied	1975-1981; 2001-2005; 2009-2021

Willamette Falls Fish Ladder[e]	Oregon Department of Fish and Game	O1	WR-43	45.354	-122.618	01/1985– present	Not tabulated; Daily, with gaps	± 0.2 ºC	-0.3 to 0.3 ºC, based on monthly difference with Portland	1985-1999; intermittently thereafter
Saint Johns Bridge[f]	City of Portland, BES	C1	WR-9	45.585	-122.765	7/1992 – 9/1999	Every 30 minutes	± 0.01 ºC	Very biased; not used.	
Saint Johns Railroad Bridge[f]	City of Portland, BES	C2	WR-11	45.5773	-122.747	9/1997– 9/2015	Every 15 minutes	± 0.01 ºC	Averaged with USGS record	1999-2012
Albany	USGS Gauge 14174000	AL	WR-192	44.6388	-123.107	08/2001– Present	Daily Max, Min & Mean	±0.05 ºC		

Notes: Stations ordered by start date, with earliest measurements first. All times given in local standard time. Bias corrections are subtracted from raw measurements on a monthly basis to obtain daily minimum; a positive value indicates a downward adjustment. Coordinates provided in the North American Datum of 1983. The locations for the measurements at Stark Street, Astoria Downtown, Willamette Fish ladder and the City of Portland measurements are estimated based on available data. River km are the thalweg distance from the mouth of the Willamette, except for Astoria which is on the Columbia River.

Specific Footnotes: (a) Measurements obtained from US National Archives; see Talke et al., 2020; (b) Measurements obtained from National Centers for Environmental Information; (c) Data obtained from NOAA; Grab samples from 1925–1995, approximately daily, generally between 10:00am–1:00pm; median ~11:30 am.(d) Data obtained from US EPA Storet database. Measurements often made from bridges in the Portland Metro area, including the Hawthorne Bridge, the Steel Bridge, and SPSS Railway Bridge. Samples pre-1960 discarded because of lack of time stamp. Grab samples after 12:00 pm (noon) not considered to avoid afternoon heating signal. Pre-12:00 pm data adjusted to daily minimum on monthly basis based on modern USGS data. Measurements at 1– 3 day frequency in 1964– 1972; (e) Data from 1985– 1999 obtained directly from agency; post 1999 records available online. Based on a comparison using 2001-2004 data, an average warming of 0.2 to 0.3 ºC occurs between Willamette Falls and Portland from July to September. A cooling of up to 0.3 ºC occurs between March to May. Little variation occurs at other times; (f) Obtained directly from agency; pre-2000 data also obtained from Berger et al., 2004.

Table 2: Meteorological stations used to develop statistical models, and associated root mean square error (RMSE) of T_w obtained for different calibration periods (annual, summer, and winter). The RMSE represents either the daily or monthly averaged difference with in-situ T_w measurements, in degrees Celsius. Station Identification numbers (ID) are from the US National Weather Service. Measurement dates denote the time period that daily maximum temperature was recorded at the given location. The latitude/longitude value for Eola (near Salem, Oregon) is estimated. All stations except Vancouver are in Oregon.

Model Name	Air temperature dataset used in model	Station ID	Dates modeled	latitude	longitude	Calibration Period	RMSE Annual Calibration (ºC)	RMSE Summer Calibration (ºC)	RMSE Winter Calibration (ºC)	RMSE Annual (monthly avg) (ºC)	RMSE Summer (monthly avg) (ºC)	RMSE Winter (monthly avg) (ºC)
1881D	Portland Downtown	USW00024274	1874–1902	45.5166	-122.6667	1881–1890	1.1	1.2	0.87	0.78	0.92	0.5
1941D	Portland Downtown	USW00024274	1902–1973	45.5333	-122.6667	1941–1952	0.91	0.68	0.75	0.62	0.48	0.43
1941A	Portland Airport	USW00024229	1938–2021	45.5958	-122.6093	1941–1952	0.91	0.66	0.78	0.6	0.46	0.42
2000A	Portland Airport	USW00024229	1938–2021	45.5958	-122.6093	2000–2015	0.88	0.51	0.75	0.62	0.31	0.48
2000D	Portland KGW[2]	USC00356749	1973–2021	45.5181	-122.6894	2000–2015	0.87	0.53	0.72	0.62	0.33	0.46
1941V	Vancouver, Washington[3]	USC00458773	1849–1868 1891–1966	45.6333	-122.6833	1941–1952	0.98	0.75	0.85	0.68	0.54	0.48
1881E	Eola	US Signal Service Observation	1870–1892	44.9323	-123.1198	1881–1890	1.22	1.41	1.05	0.91	1.17	0.72

Notes:

1. The annual RMSE between measurements and the climatological average is 1.86, 1.46, and 1.43 ºC for the 1881–1890, 1941–1952, and 2000–2015 calibration periods, respectively.
2. The 1973–1999 measurement was at a slightly different location of (45.517W, -122.683E). The elevation of the 1973–present dataset is ~48.5m. The lapse rate for the standard atmosphere (6.5 ºC per 1000m) suggests that the difference to a measurement at sea-level is ~0.3 ºC. An observed difference in average daily maximum temperature at the Portland Airport (17.46 ºC, <10m relative to sea-level) and Portland KGW (17.07 ºC) between 2000–2020 is therefore mostly caused by elevation differences.
3. The Dec. 1849–1868 measurement at Fort Vancouver was made by the US Signal Service; the approximate location was 45.633N, - 122.65E, and was several km east of the 1891–1966 measurement. The gauge was moved in 1966 to a higher elevation location with a known bias (Mote et al., 2002). The 1966–present data is therefore not used.

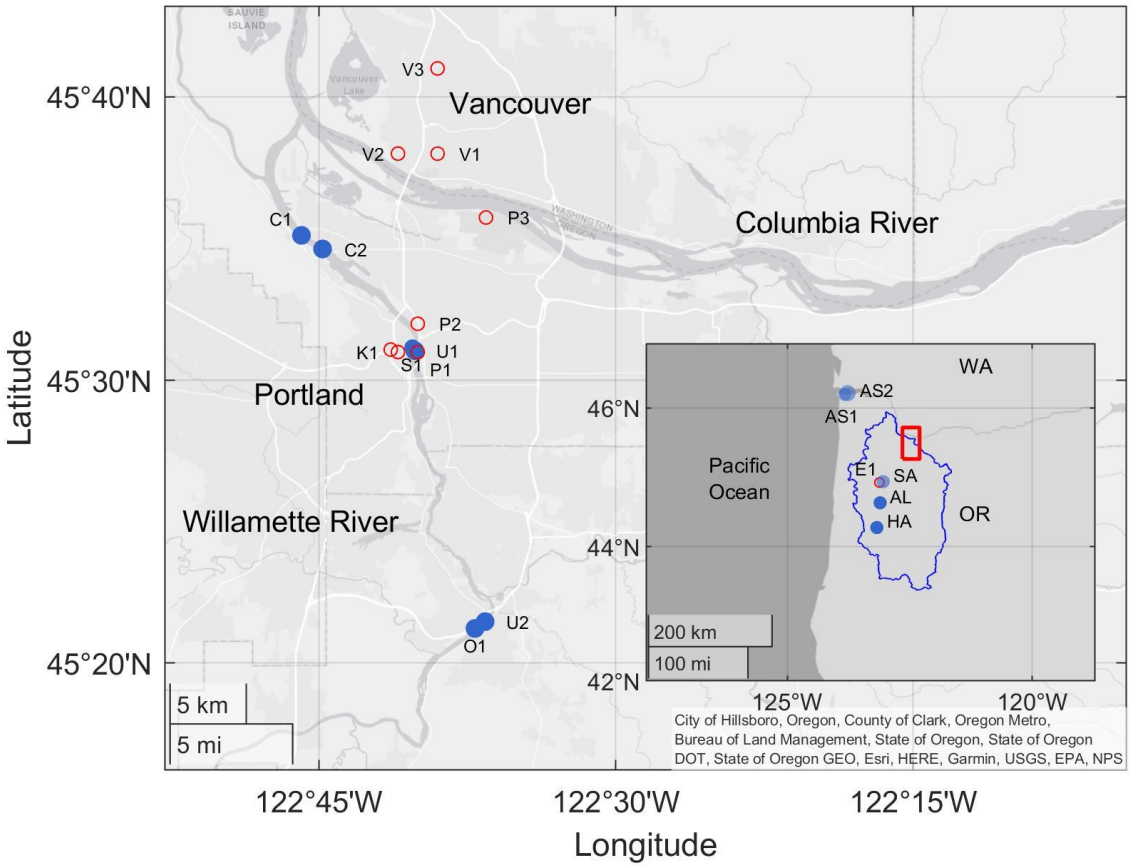

Figure 1: Site map with locations of T_w (blue, closed circles) and T_a (red, open circles) measurements. The red bounding box in the inset denotes the Portland/Vancouver Metropolitan Area depicted in the larger figure. The Willamette River watershed boundaries are denoted in blue. OR = Oregon, WA = Washington. Abbreviations and period of record of the measurements are provided in Table 1.

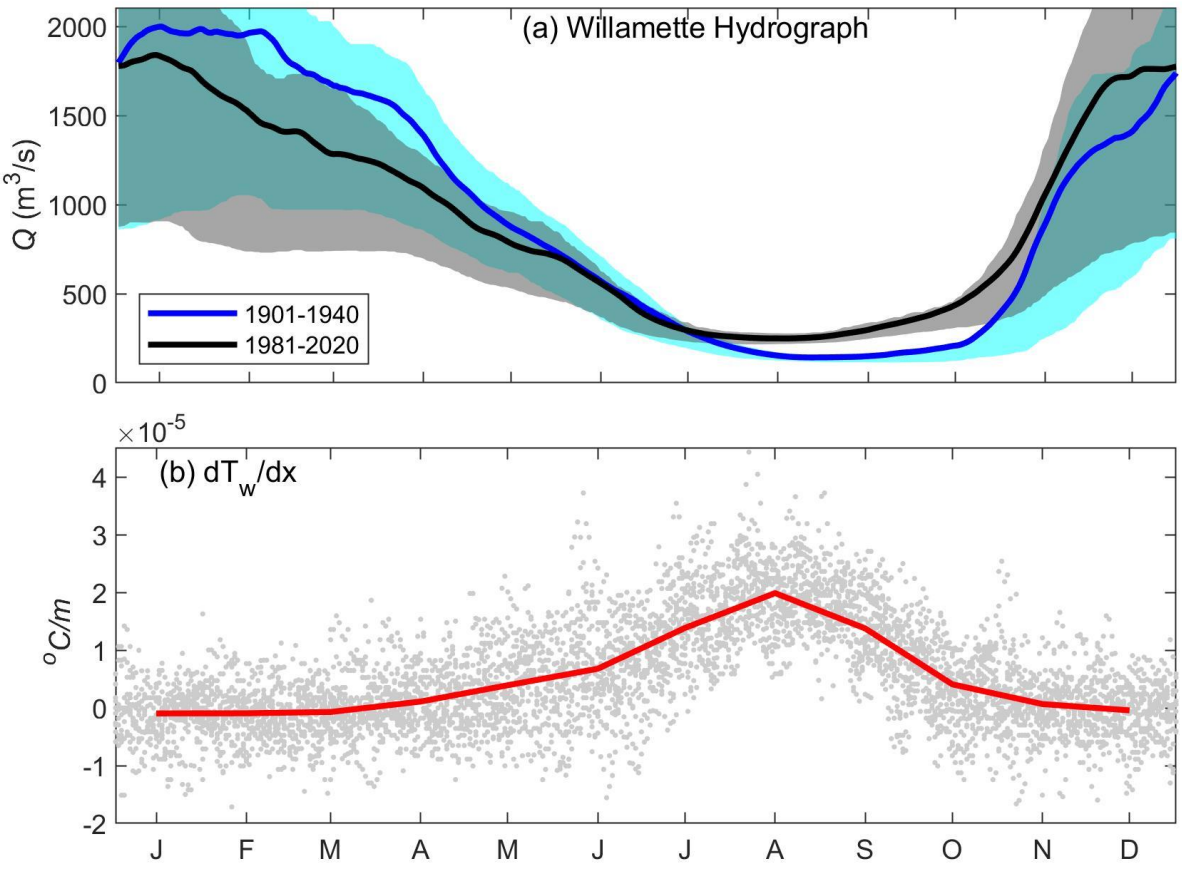

Figure 2: (a) The Willamette hydrograph at Portland, Oregon for the pre-reservoir (1901–1940) and modern (1981–2020) periods, and (b) the horizontal T_w gradient between Albany, Oregon and Portland Oregon for the 2000–2017 time period. Positive indicates that downstream measurements in Portland are warmer. Shading in (a) denotes the 25th and 75th percentile of measured discharge. The along-river distance between Portland and Albany is 169 km. The red line in (b) denotes the monthly average. Tick marks denote the middle of each month.

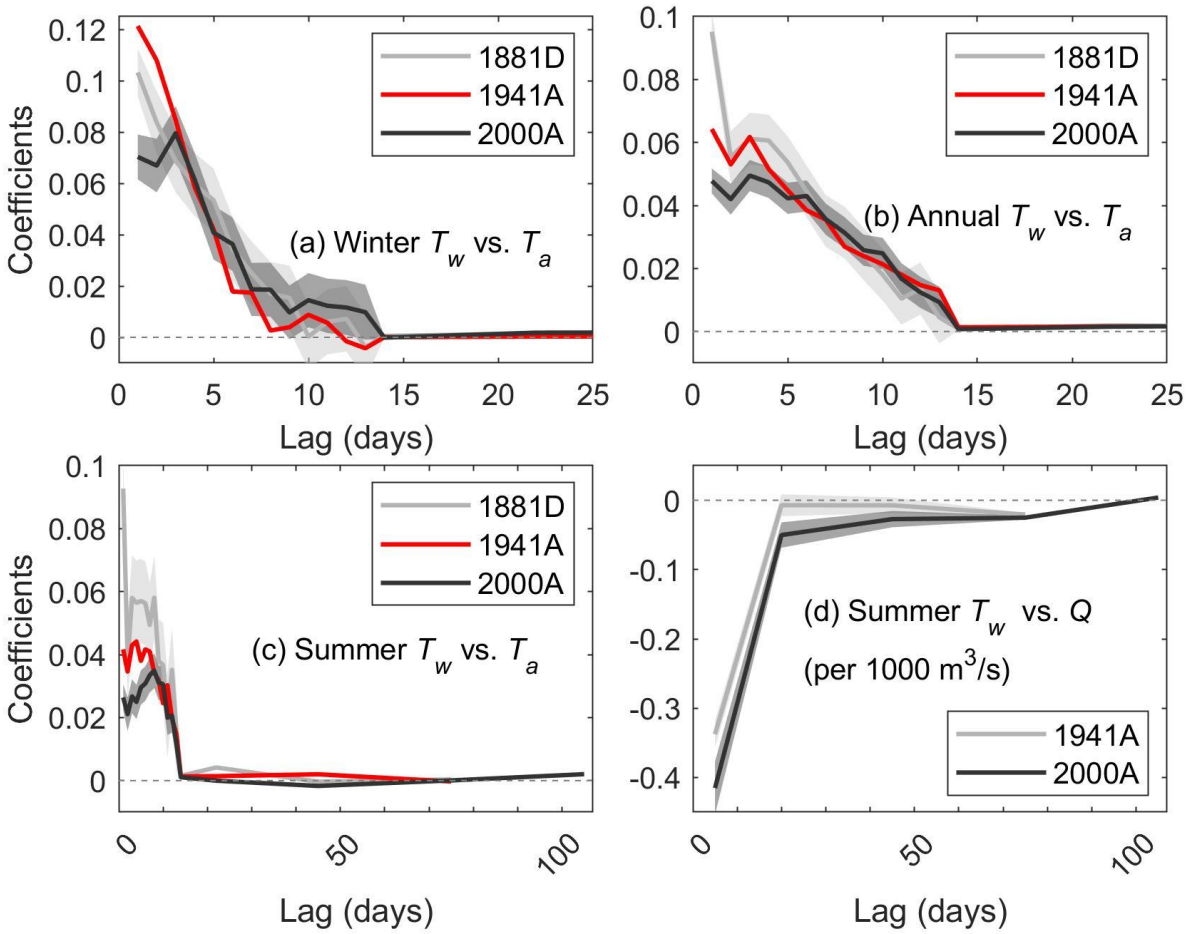

Figure 3: Coefficients for statistical model vs time lag for (a) T_a in the winter model (Nov– Mar); (b) T_a in the annual model (all months); (c) T_a in the summer model (July– Sept) and (d) discharge Q in the summer model (July– Sept). The 1881 model is calibrated to 1881– 1890 T_w data, the 1941 model is calibrated to 1941– 1952 T_w data, and the 2000 model is calibrated to 2000– 2015 T_w data. The letter denotes whether T_a data was sourced from Downtown Portland (D) or from the Airport (A). Similar results are found for the model based on Vancouver T_a data (not shown). No statistically significant effect of river discharge was found for winter or annual models, and the 1880s summer model, and are not shown.

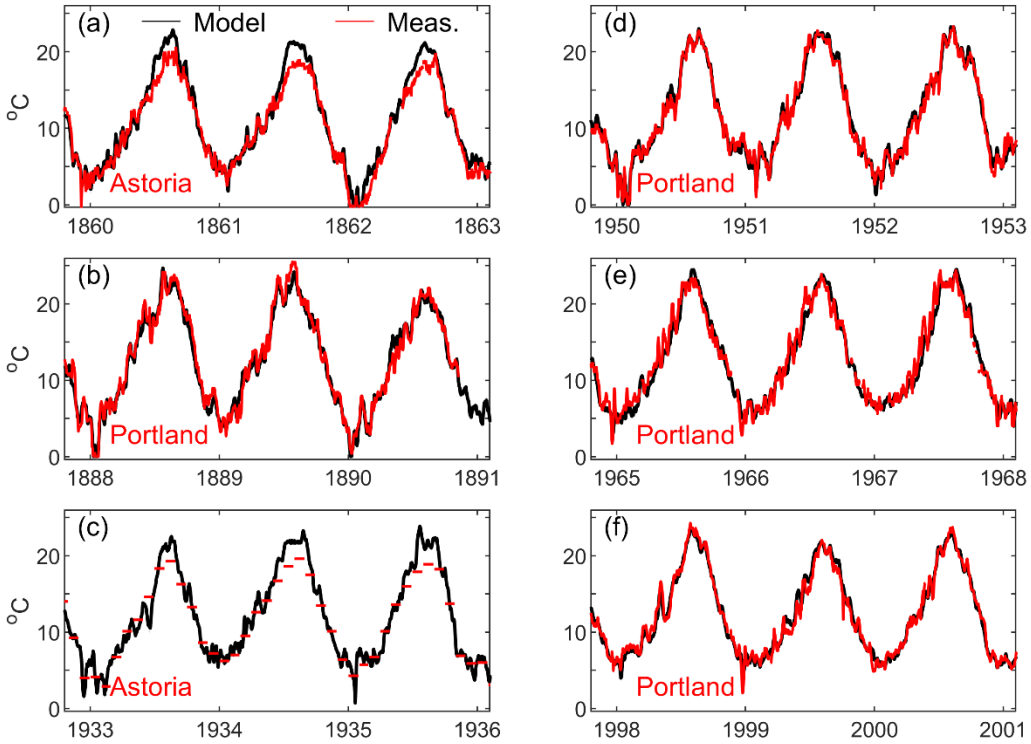

1151

1152 Figure 4: Comparison of modeled and measured T_w for six, three-year periods. The composite
1153 Portland T_w is used in (b), (d), (e) and (f), while Astoria measurements are used in (a) and (c).
1154 Only monthly averages of T_w are available at Astoria from 1925 to 1940 and 1943– 1948 (see
1155 Table 1). Black is modeled, red is measured.

1156

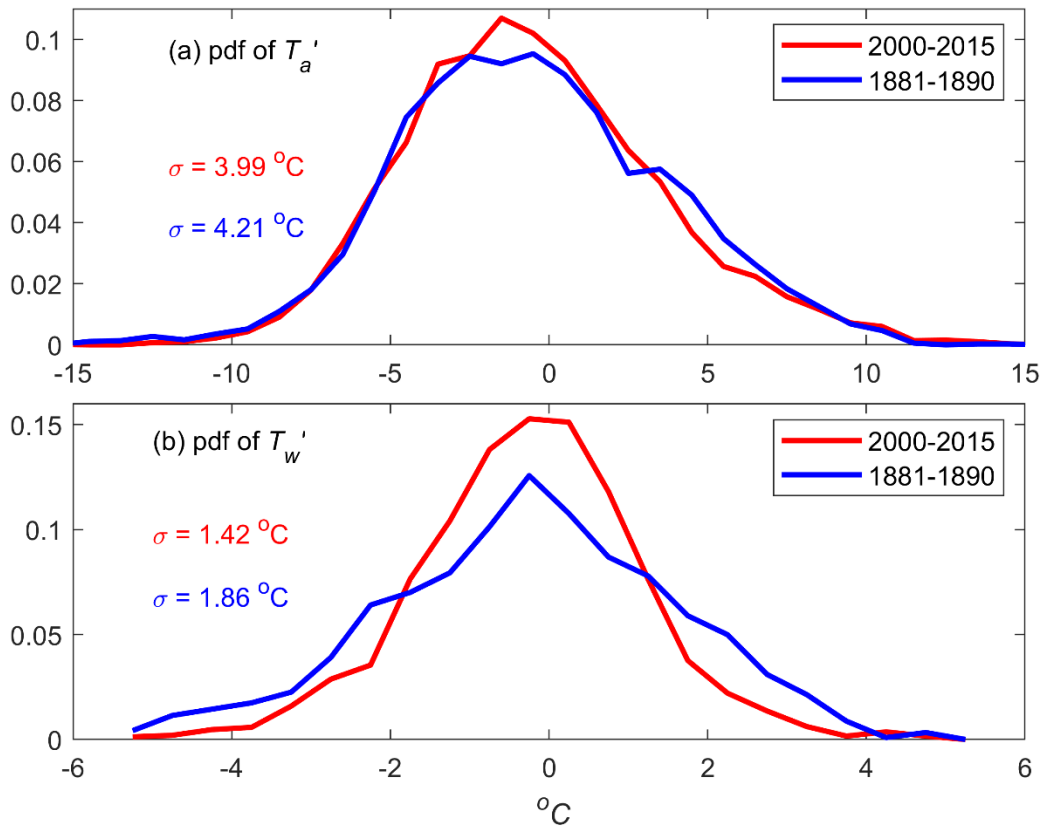

1157

1158 Figure 5: The measured probability density function (pdf) and standard deviation σ of T_a and T_w
1159 anomalies for the 1881–1890 and 2000– 2015 periods. The anomalies (T_a' and T_w') are defined
1160 as the deviation from the 30 day climatological mean (see Equation 5 & 6). The y-axis gives the
1161 probability density.

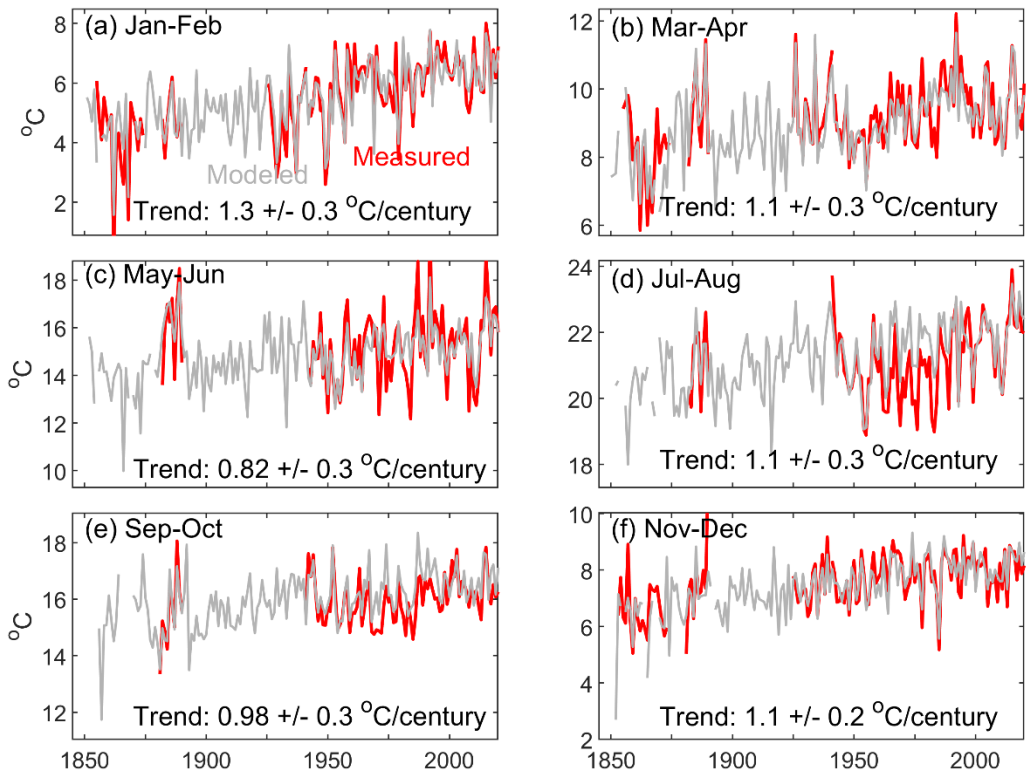

1162

1163 Figure 6: Seasonal trends in water level, averaged over two-month water periods. Measure-
1164 ments (red) and model results (grey) are correlated. The trends and 95% confidence interval are
1165 based on a linear regression to model results, 1850–2020; November–April data for 1854–1876
1166 are from Astoria (see Talke et al., 2020). Note different y-axis scales.

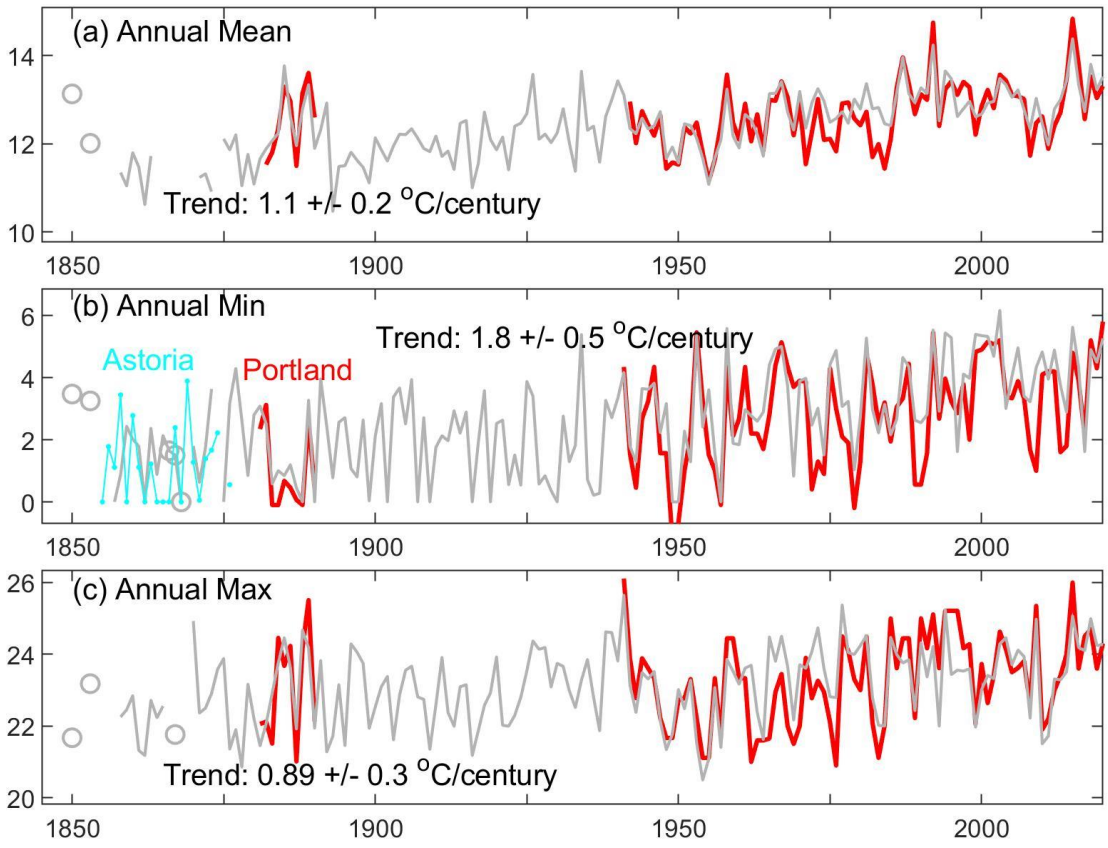

Figure 7: Time rate of change of annual mean, annual minimum, and annual maximum T_w. Grey denotes model data, red denotes data from Portland region, and cyan denotes T_w measurements in Astoria (annual minimum only, panel b). The trend is calculated by regression fit to model results over the 1850–2020 period. Evaluation is based on daily minimum T_w (see section 2). Years in the 1850s and 1860s without sufficient model data are excluded.

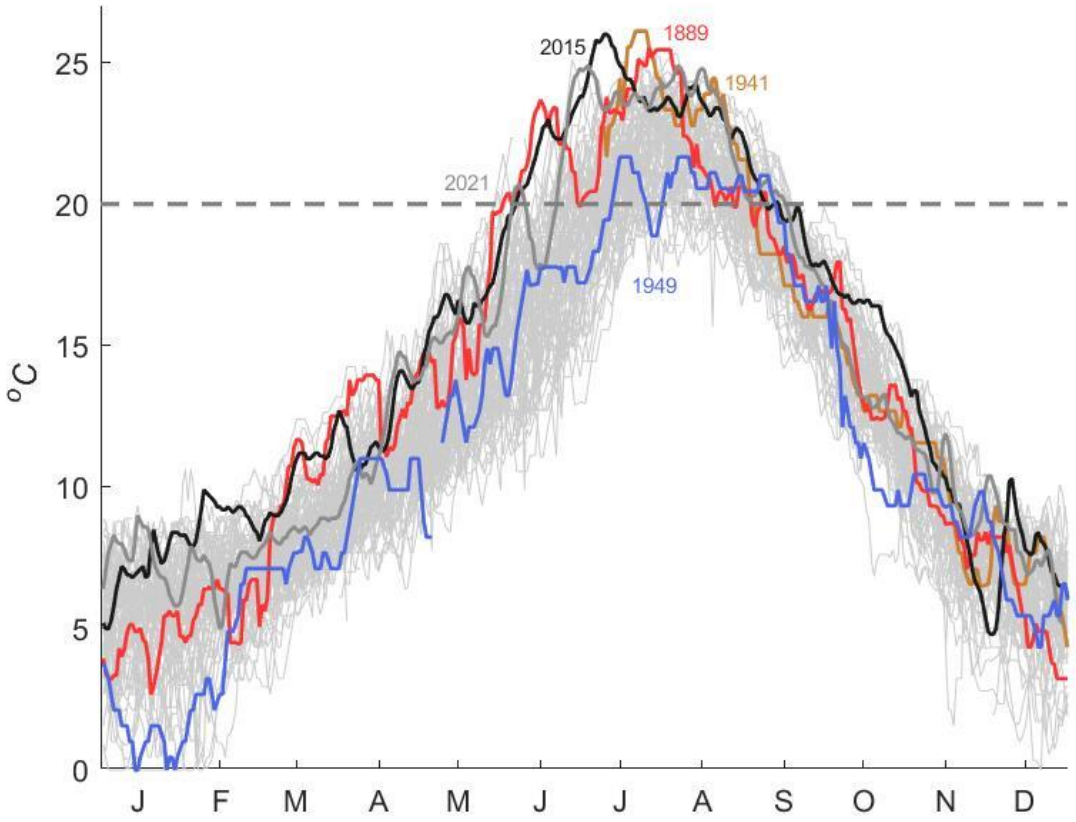

Figure 8: Spaghetti plot of all measured T_w data from between 1881–1890 and 1941–2021. Five years (1889, 1941, 1949, 2015, and 2021) are colored as labeled for comparison. The tick marks on the x-axis denote the middle of each month.

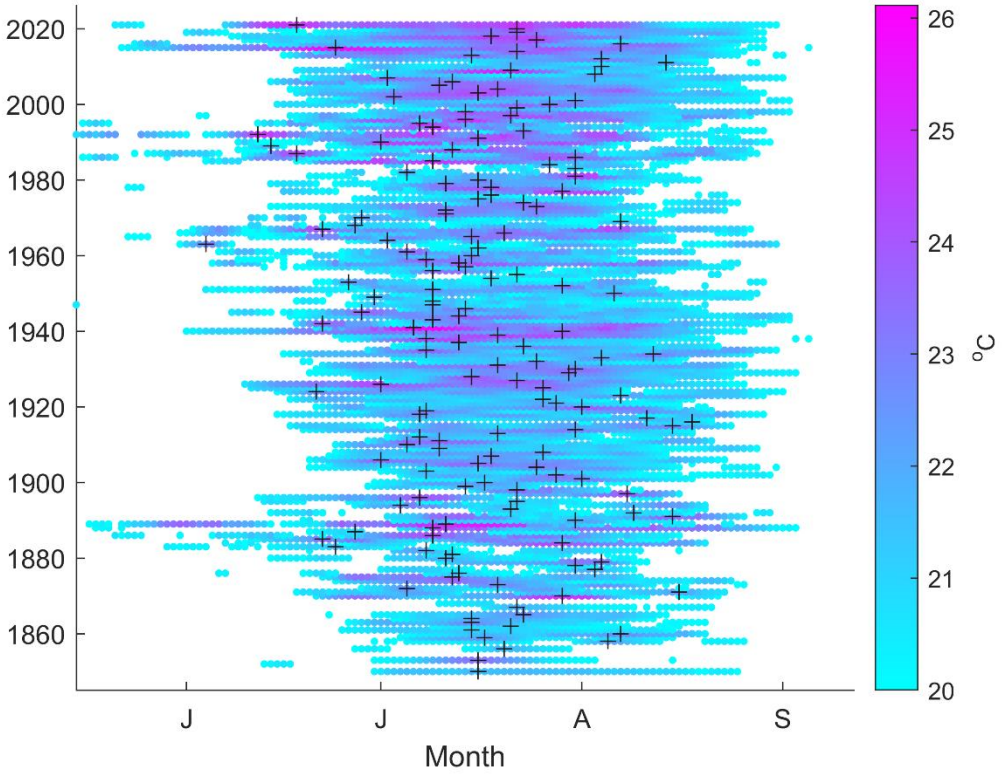

Figure 9: Summertime Willamette River T_w exceedances of 20 ºC, 1850 to 2021. The instrumental record is used between 1881 and 1890 and 1941 to 2021, and the remainder is infilled with modeled T_w. Crosses denote the time of the peak annual T_w. Missing T_a data precluded peak estimates for 1851–1852, 1854–1855, 1857, 1866, and 1868–1869 (see supplemental data). The tick marks on the x-axis denote the middle of each month.

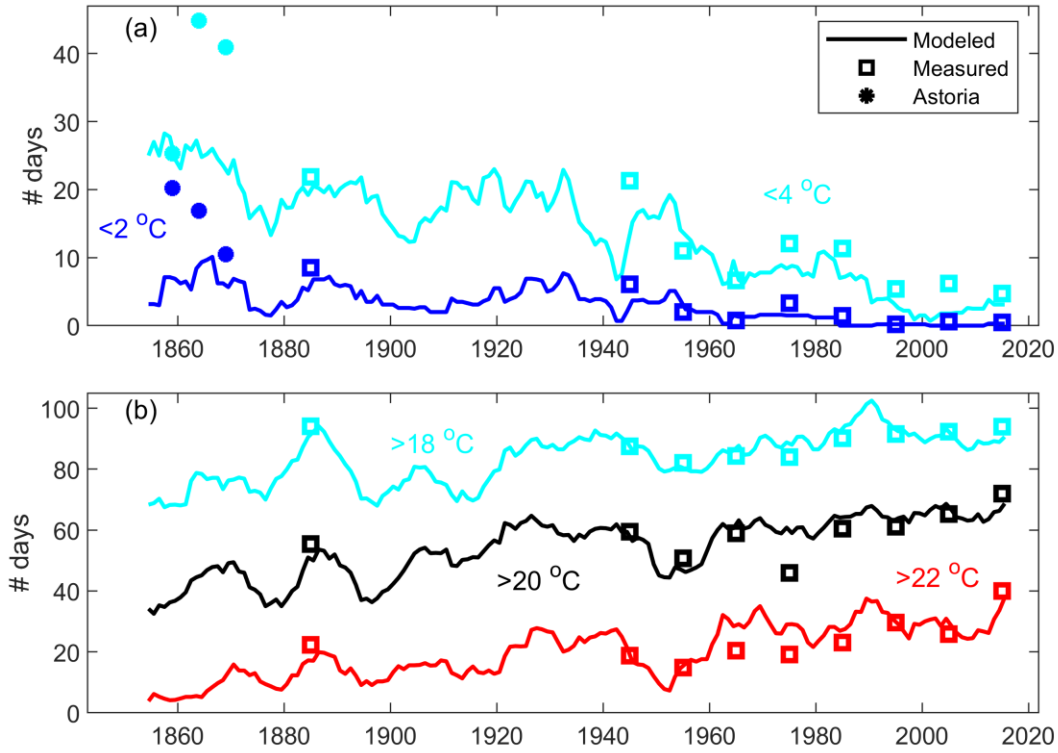

Figure 10: Comparison of the modeled and measured number of days per year from 1850 to 2020 that T_w is (a) below thresholds of 2°C or 4°C and (b) above thresholds of 18°C, 20°C, or 22°C. Square symbols denote the 10-year average based on measurements, while the solid line is a running 10-year average of modeled T_w. Measurements based primarily on bias-corrected upstream gauges (1962, 1983–1984) are excluded. Grey shading is the 95% confidence interval, based on resampling of model coefficients using a Monte-Carlo based technique. Wintertime measurements from Astoria (1854–1876) are included in (a) for comparison.

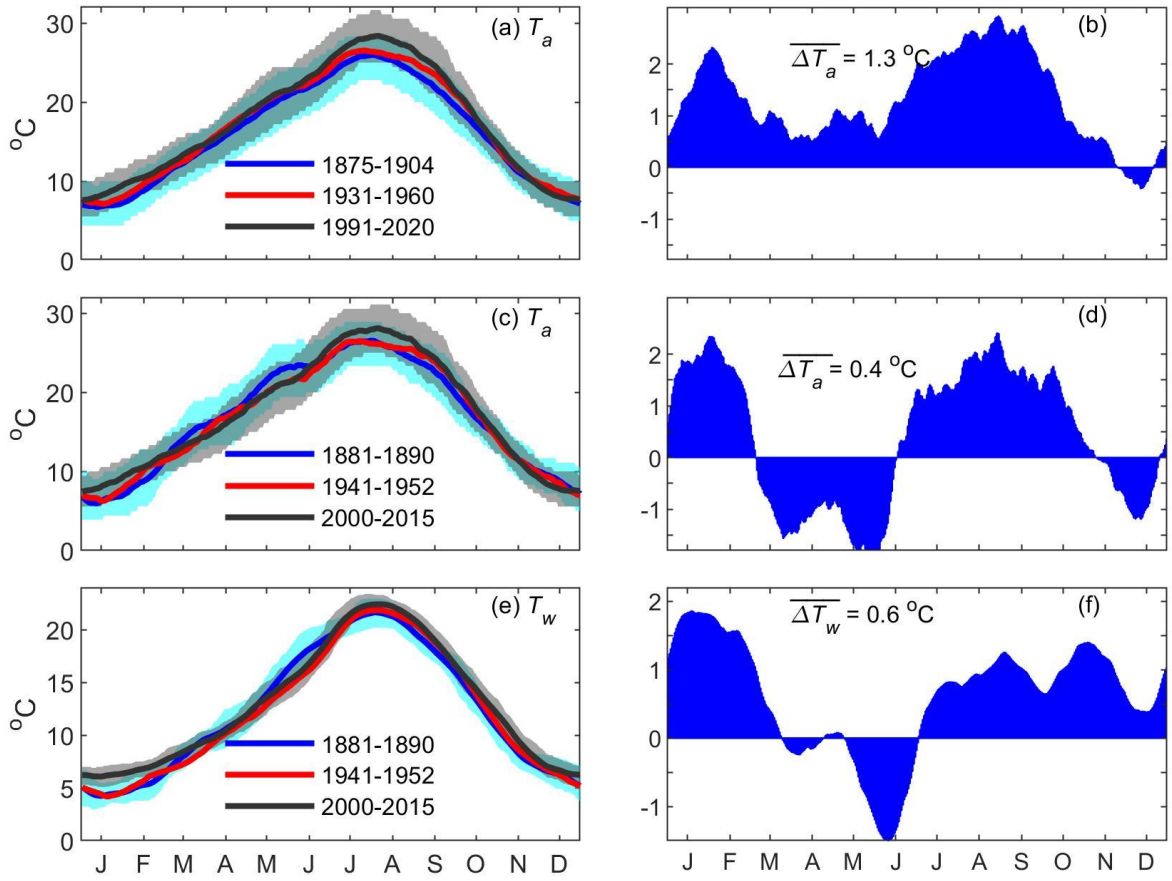

Figure 11: T_a and T_w climatology in Portland (a,c,e) and the corresponding difference between the modern and historical periods (b,d, e). The T_a difference plot in (b) and (d) is the difference between late 19th and early 21st century air temperature data in (a) and (c), respectively. The difference in (f) is the difference between 2000-2015 and 1881-1890 T_w data. Climatology is determined using a 30d moving average; shading denotes the 25th and 75th percentile of the measurements. A 30-year average is used in (a); the time periods for (c) and (e) are determined by the time period used to calibrate the T_w model. The tick marks on the x-axis denote the middle of each month. The average difference between the modern and earliest period is provided in (b,d,e).

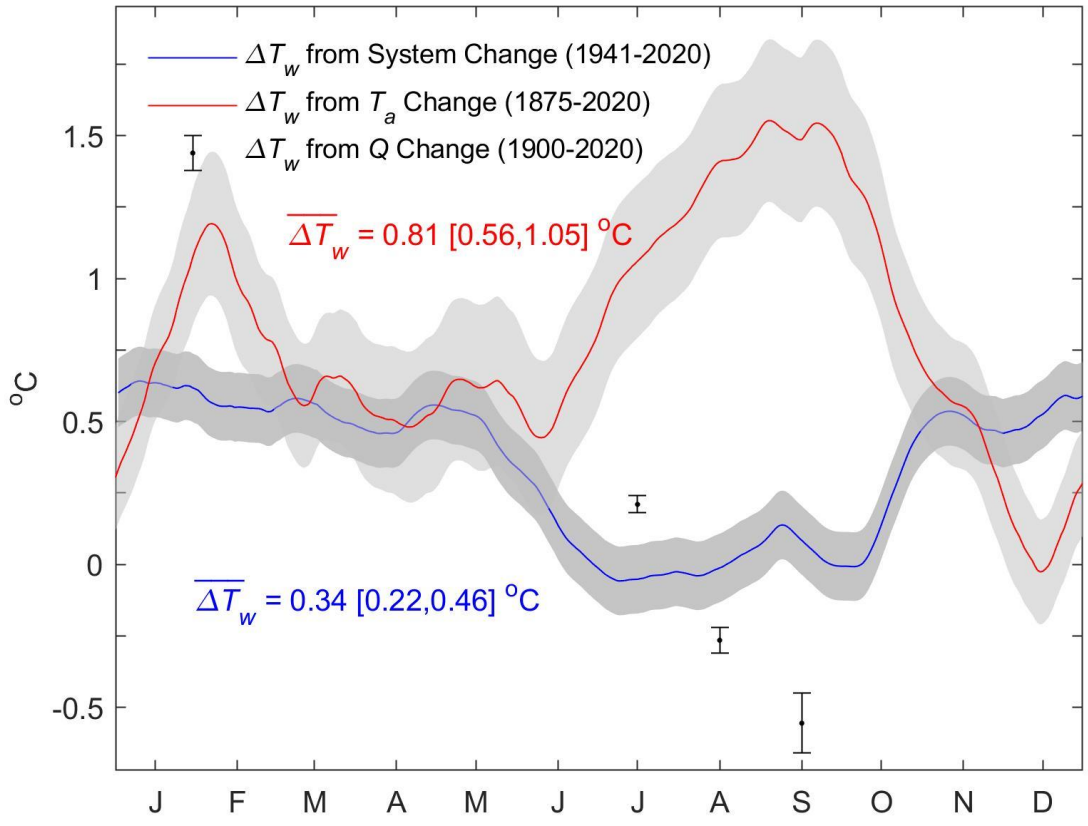

Figure 12: Estimated T_w changes caused by T_a (climate change), system changes (i.e., differences between the parameters of the modern and historic models), and discharge changes (July–September). A positive value indicates an increase over time. Shading shows 95% uncertainty bounds and is a combination of the uncertainty in the mean climatology and the model coefficients. The uncertainty bounds for the influence of altered river flow denote the difference in the 1941A and 2000A model estimates. See section 2.5 for details on calculations.